

Photoionisation Modelling of the Emission Line Regions and Warm Absorbers in AGN

Sam Grafton-Waters

G. Branduardi-Raymont, M. Mehdipour, M. J. Page, E. Behar, J. Kaastra

N. Arav, S. Bianchi, E. Costantini, J. Ebrero, L. Di Gesu, S. Kaspi, G. A. Kriss, B. De Marco, J. Mao, R. Middei, U. Peretz, P.-O. Petrucci, G. Ponti

What are AGN and why should we care?

AGN – in a Nutshell

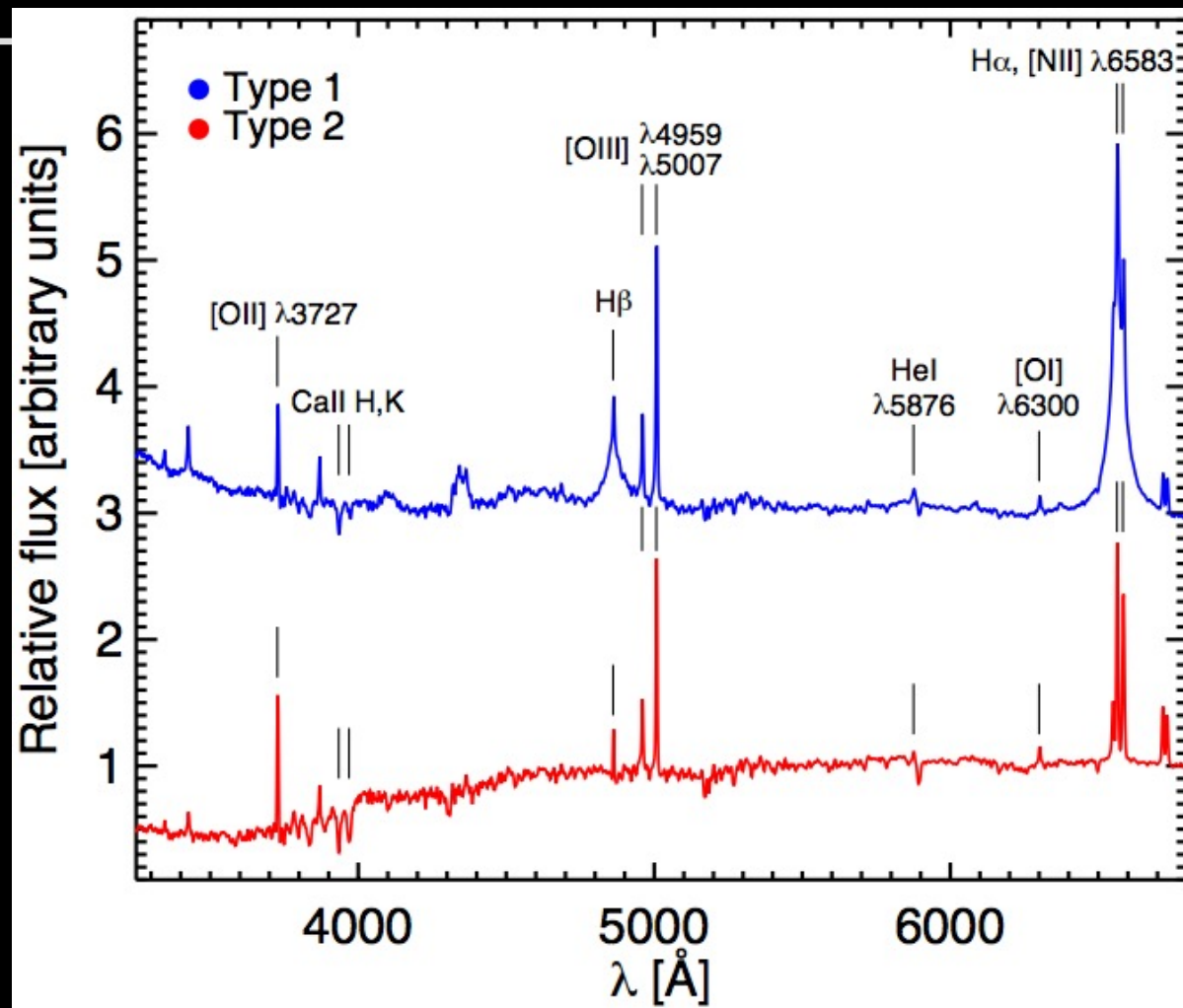
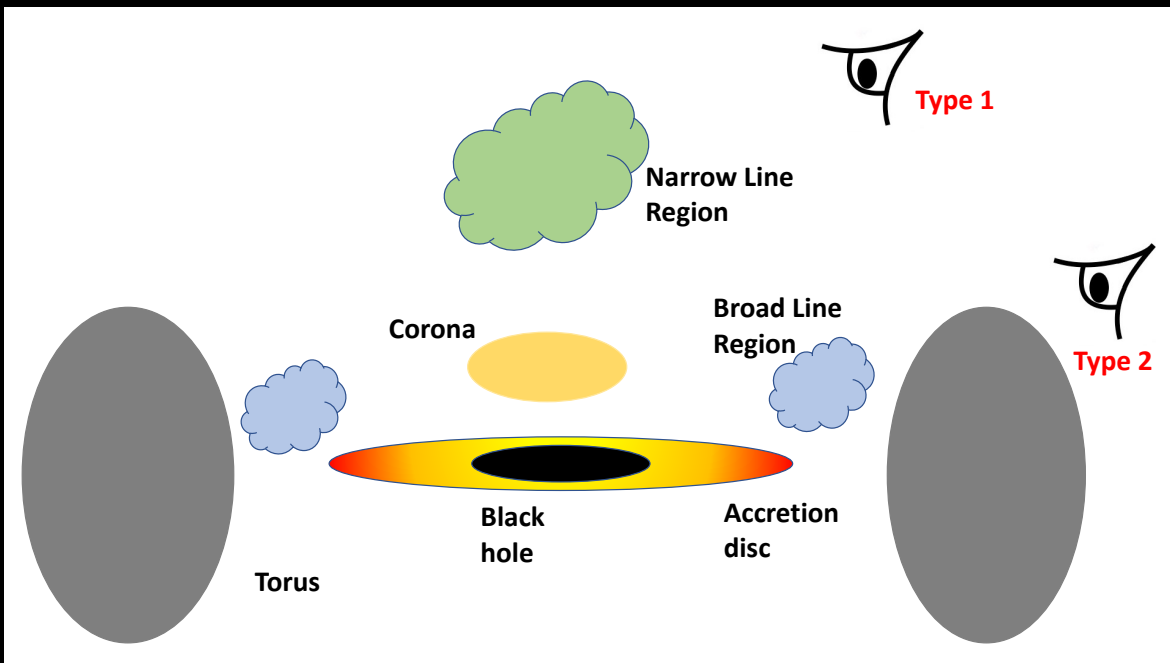
- $M_{BH} = 10^5 - 10^{10} M_{\odot}$
- $L_{bol} = 10^{34} - 10^{41} W$
- Powered via accretion
- Matter also ejected into galaxy
 - Disk winds (UFO; $v_{out} \sim 0.1 - 0.4 c$; e.g. Tombesi et al. 2010,12,13)
 - Torus Winds (WA; $v_{out} \sim 100 - 1000 \text{ km s}^{-1}$; e.g. Blustin et al. 2005)



Image courtesy: MIT Kavli Institute for Astrophysics and Space Research

AGN Unification

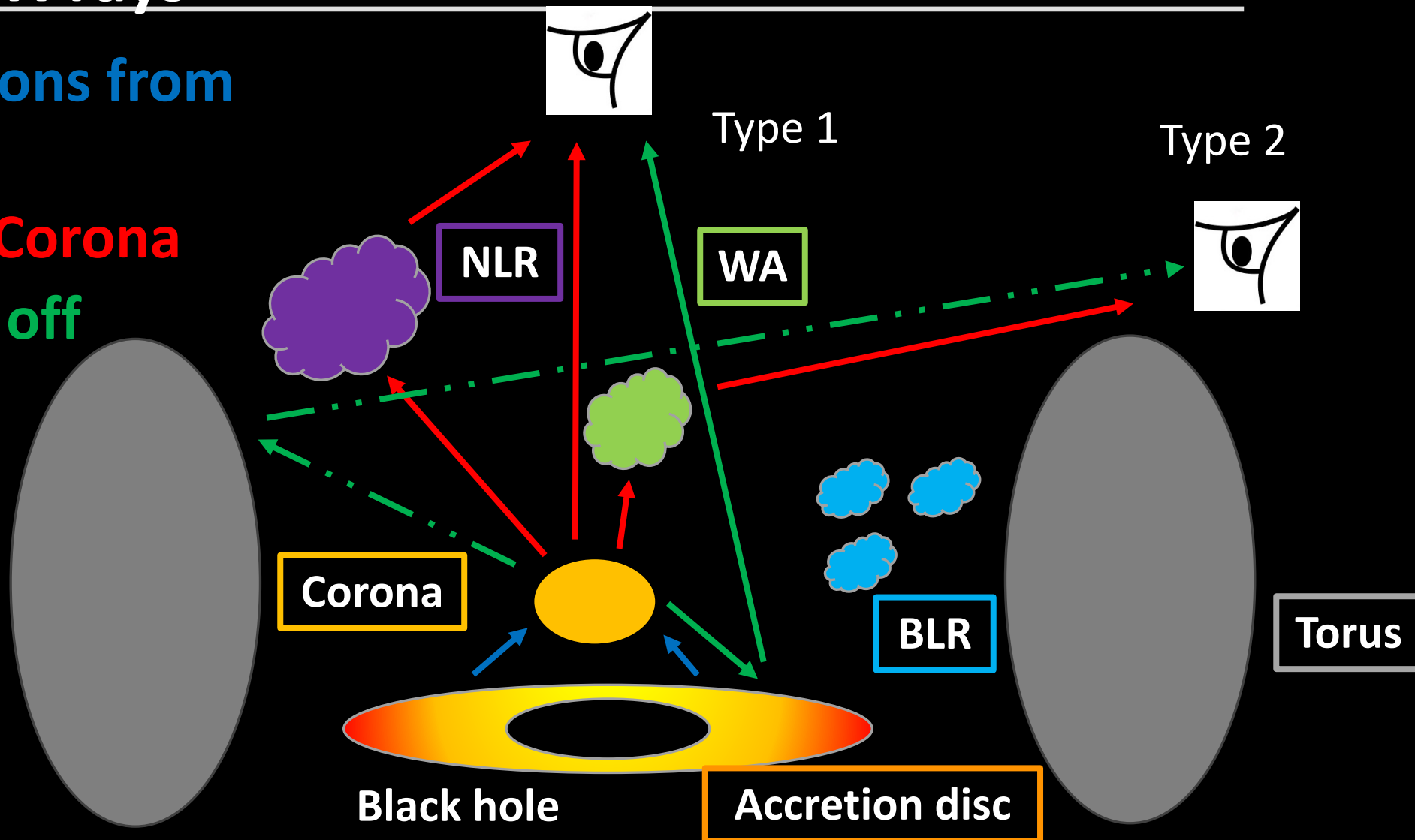
Adapted from DiPompeo et al. 2018
by Hickox & Alexander 2018



Unification Theory of AGN: Miller & Antonucci 1983;
Antonucci & Miller 1985

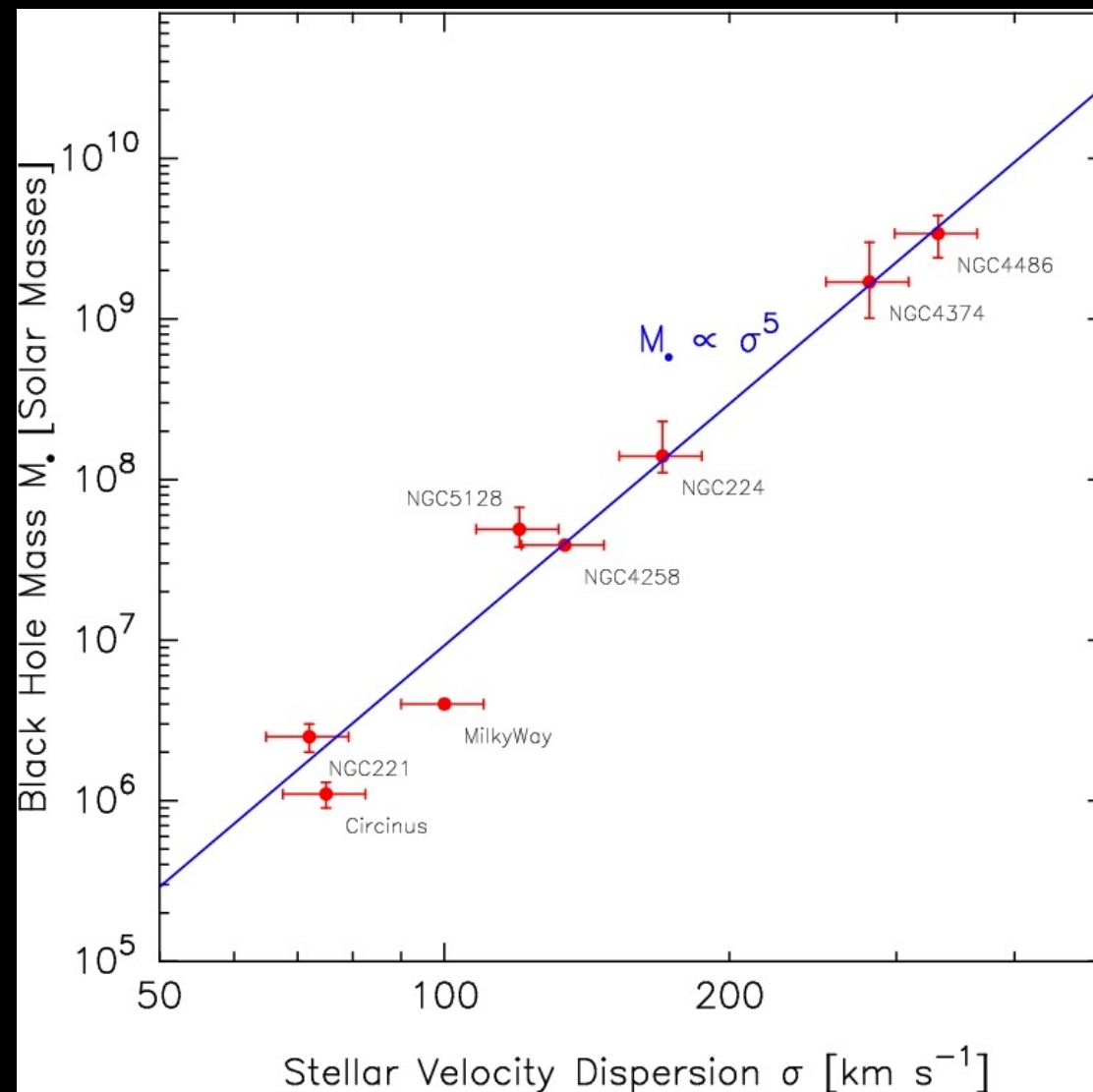
Origin of X-rays

- UV/Optical photons from accretion disc
- X-rays from hot Corona
- Reflected X-rays off the disc or torus



Motivation for studying AGN winds

- Main questions:
 - Origin of winds
 - Launching Mechanism
 - Location and Geometry
- M- σ relation
 - Galaxy impact
 - Co-evolution



Talk outline

1. Photoionisation modelling

- Photoionised Plasma properties
- Model: PION

2. Results from X-ray analysis on AGN

- NGC 5548
- NGC 3783

3. NGC 7469

- My Analysis from Multiwavelength Campaign
- Distance Measurements

4. Current work: NGC 1068

- Spectral analysis

5. Future: ATHENA



Photoionisation Modelling

PION model in SPEX

- Assume photoionisation equilibrium
 - Rate of ionisation = Rate of recombination
- State of the photoionised gas depends on the ionisation parameter ξ

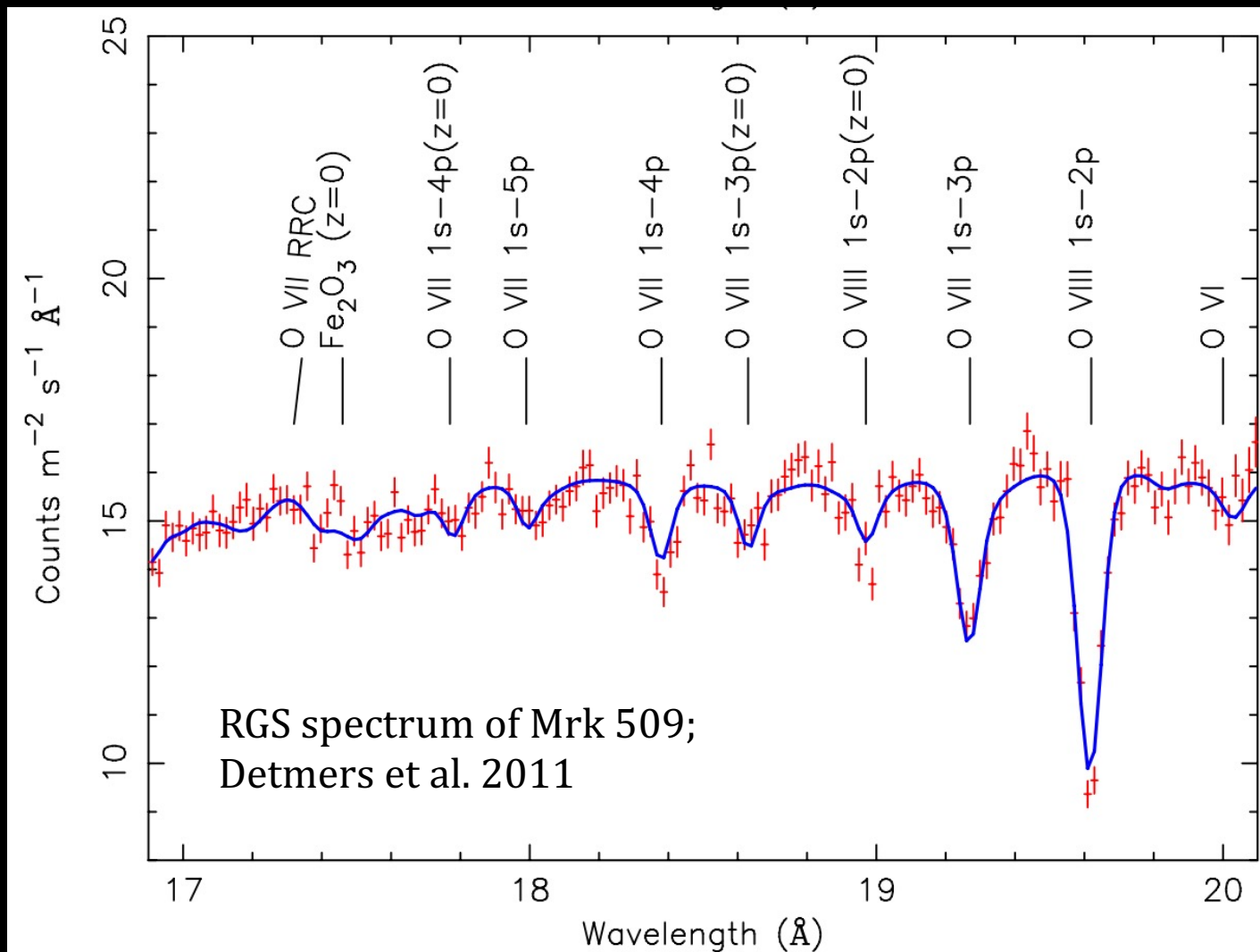
$$\xi \equiv \frac{L_{ion}}{nr^2}$$

PION

- Self consistent model (M. Mehdipour et al. 2016)
- Simultaneously models the continuum and ionised plasma
 - Requires SED of AGN
- Computes both the photoionisation solution and X-ray spectrum

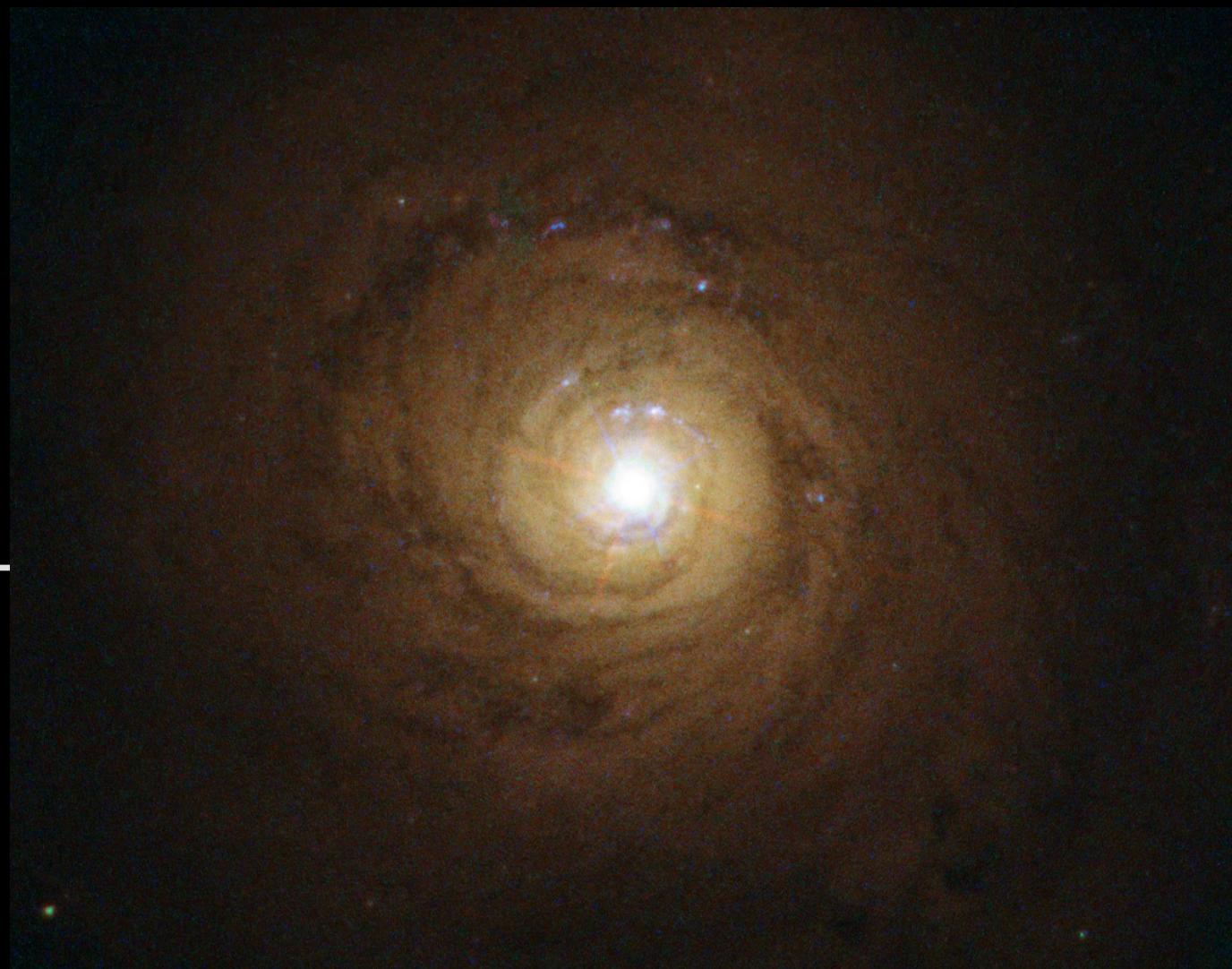


Plasma Properties



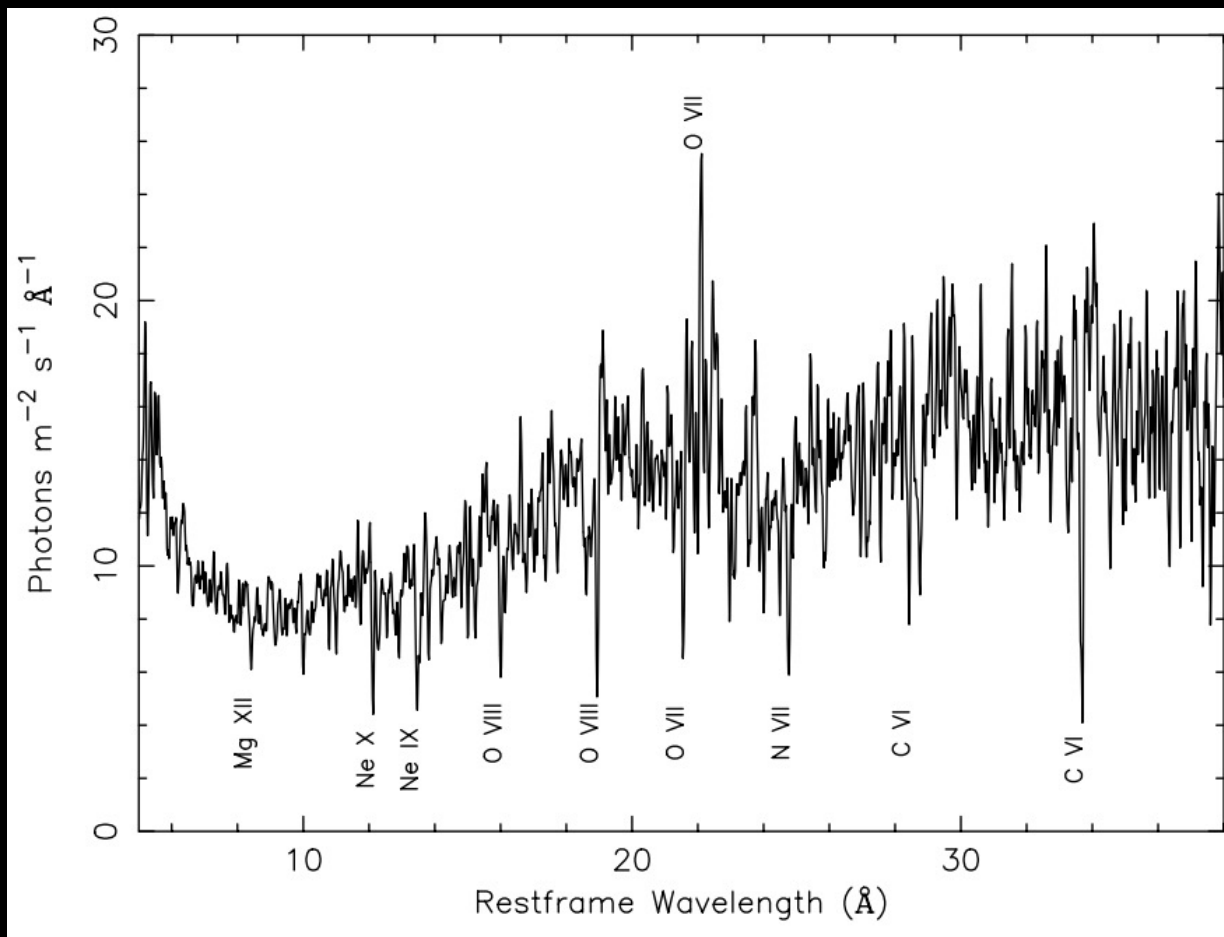
- N_H - the line depth
 - $10^{24} - 10^{28} \text{ m}^{-2}$
- $\xi \equiv \frac{L_{\text{ion}}}{nr^2}$ - ionisation
 - $\log \xi = 0 - 3$
- v_{turb} - line broadening
 - $\sim 10^1 - 10^2 \text{ km s}^{-1}$
- v_{out} - line centring
 - $> 10^2 - 10^3 \text{ km s}^{-1}$
 - Blueshifted
- **Multiple components to fit all the emission/absorption lines**

NGC 5548

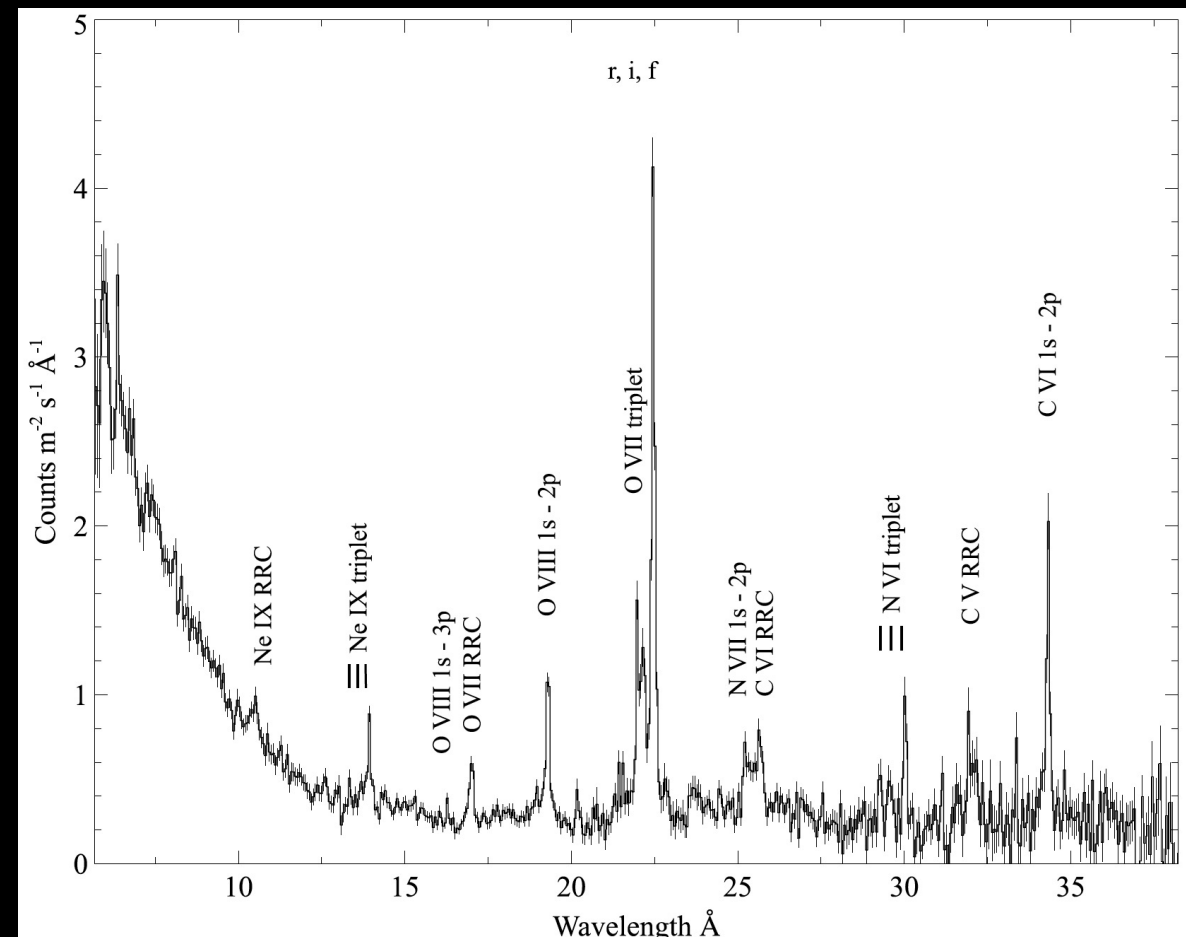


ESA/Hubble

Spectral Features

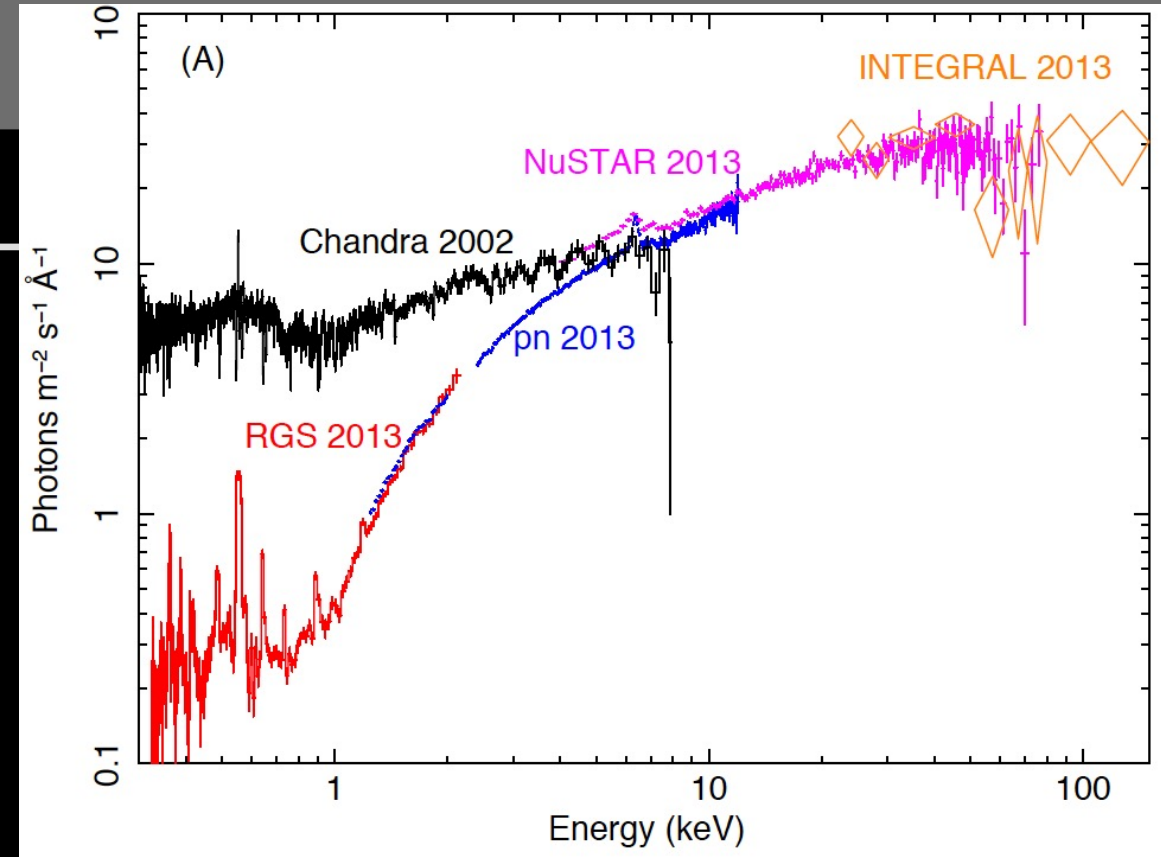
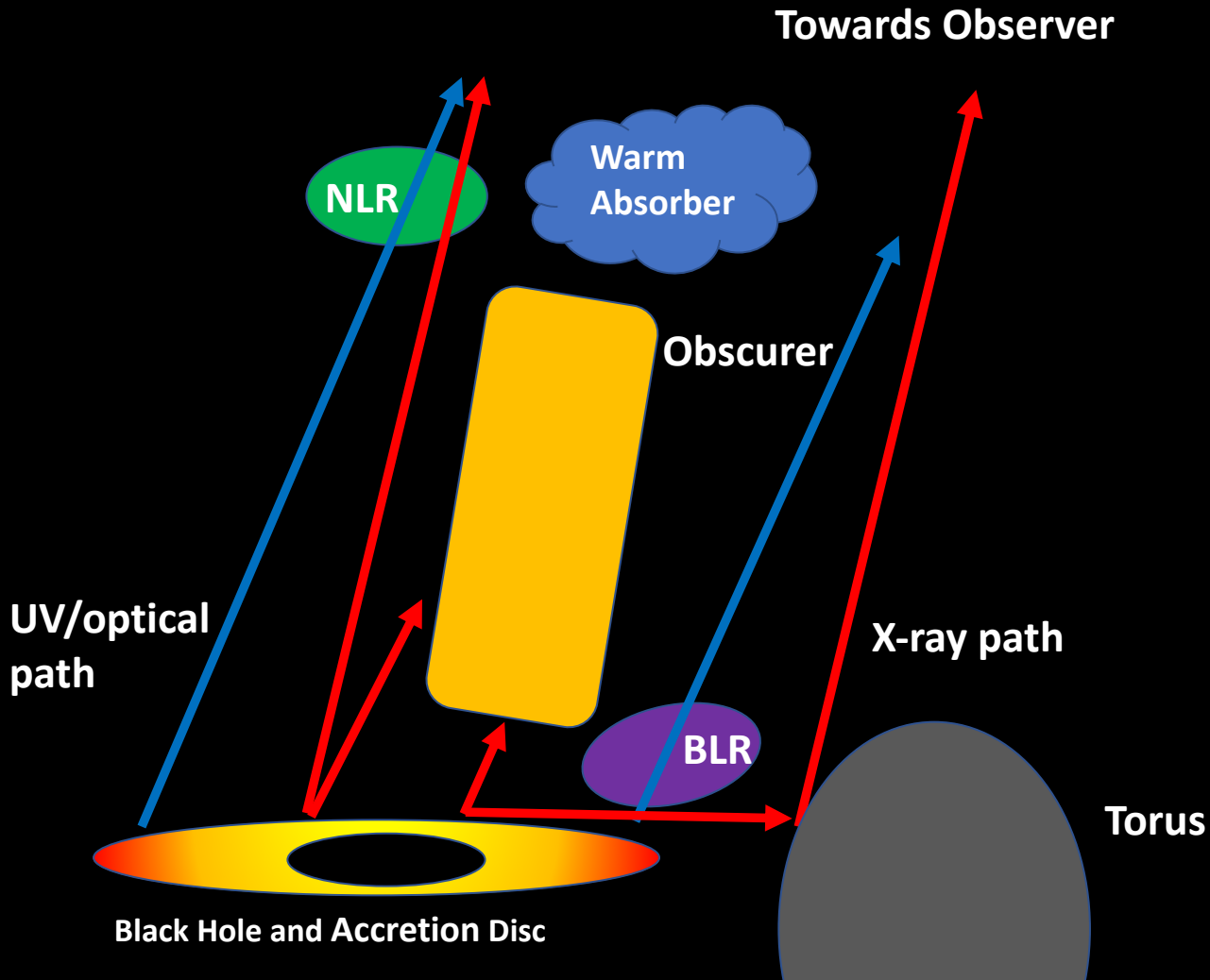


Chandra Spectrum 2000;
J. Kaastra et al 2000



RGS Spectrum 2013;
M. Whewell et al. 2015

The Obscurer

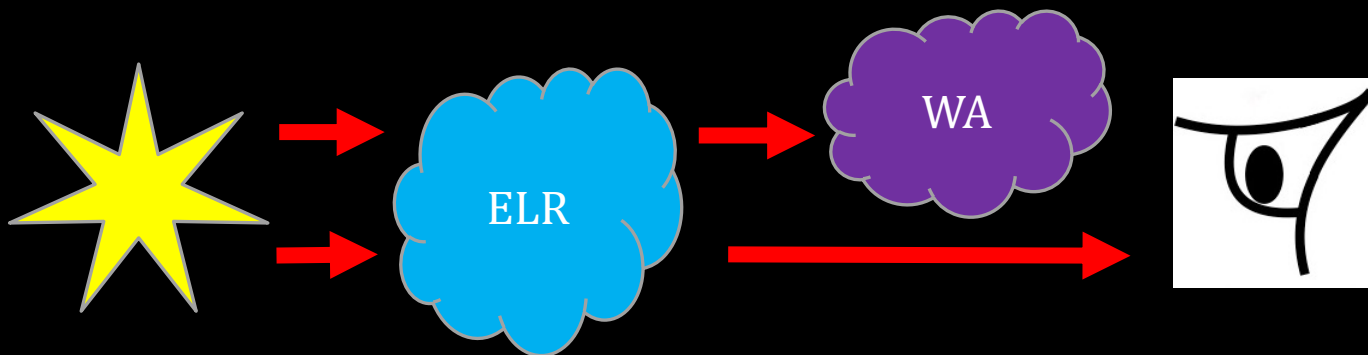


J. Kaastra et al. 2014

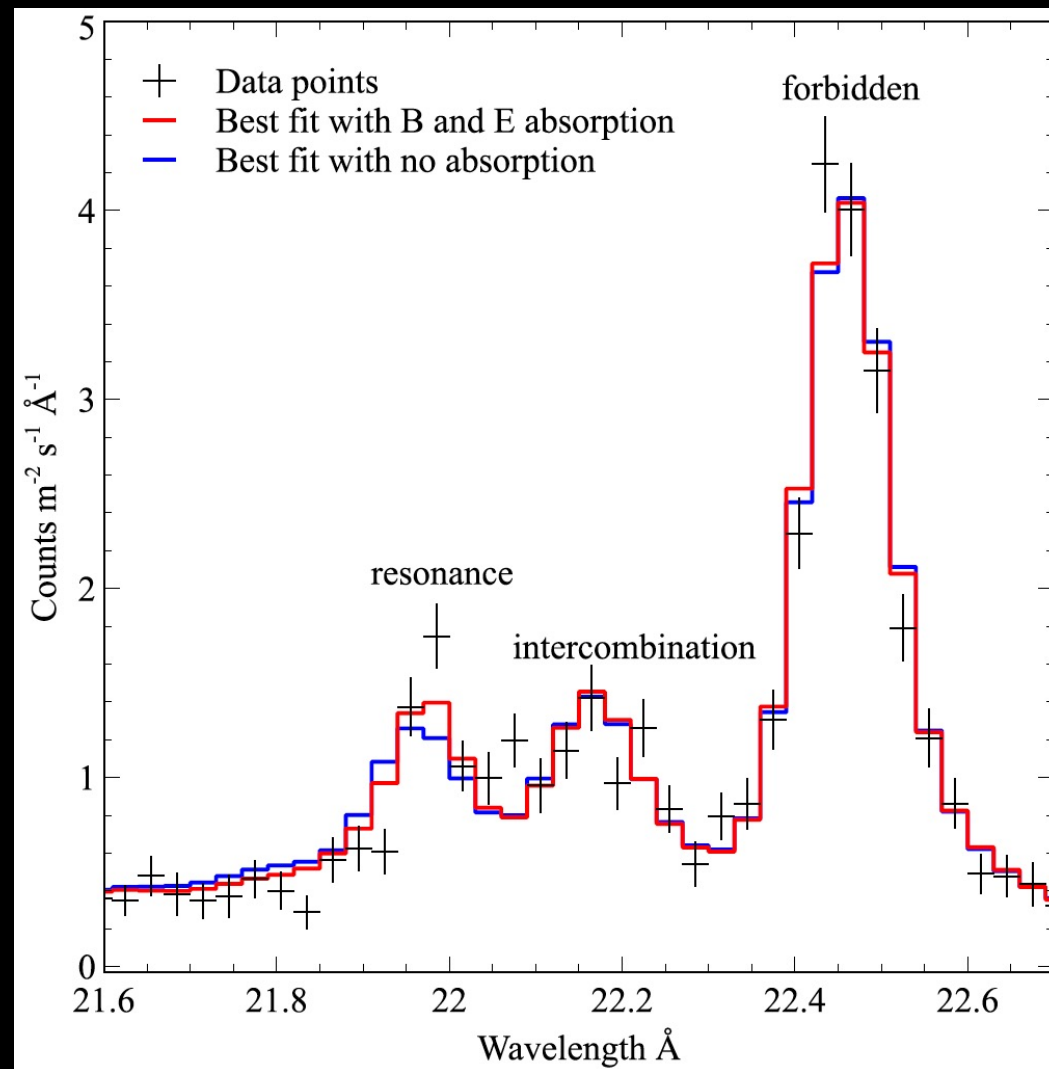
- 2 components
- $v_{\text{out}} \sim 5000 \text{ km/s}$
- Covers 80% of X-ray flux
- $r = \text{few light days}$
- Obscuration event 7+ years long

O VII Discrepancy

Line ^a	Rest λ (Å)	Measured λ ^{b c} (Å)	Flow velocity (km s ⁻¹)
O VIIr	21.602	21.601 ± 0.004	-20 ± 50
O VIIi	21.807	21.772 ± 0.020	-480 ± 160
O VIIf	22.101	22.077 ± 0.002	-320 ± 40



M. Whewell et al. 2015



Multi-Component Model

Comp.	N_H (10^{25} m^{-2})	$\log(\xi)$ (10^{-9} W m)	v_{mic} (km s^{-1})	v_{out} (km s^{-1})
EM 1	14.7 ± 0.1	1.30 ± 0.02	520 ± 40	-49 ± 6
EM 2	19.3 ± 1.3	0.14 ± 0.04	250 ± 60	-410 ± 50
EM 1	9.7 ± 1.3	1.31 ± 0.02	400 ± 30	-47 ± 4
EM 2	30 ± 7	0.13 ± 0.05	< 280	-420 ± 30
EM 3	23 ± 6	1.24 ± 0.07	100 (f)	0 (f)

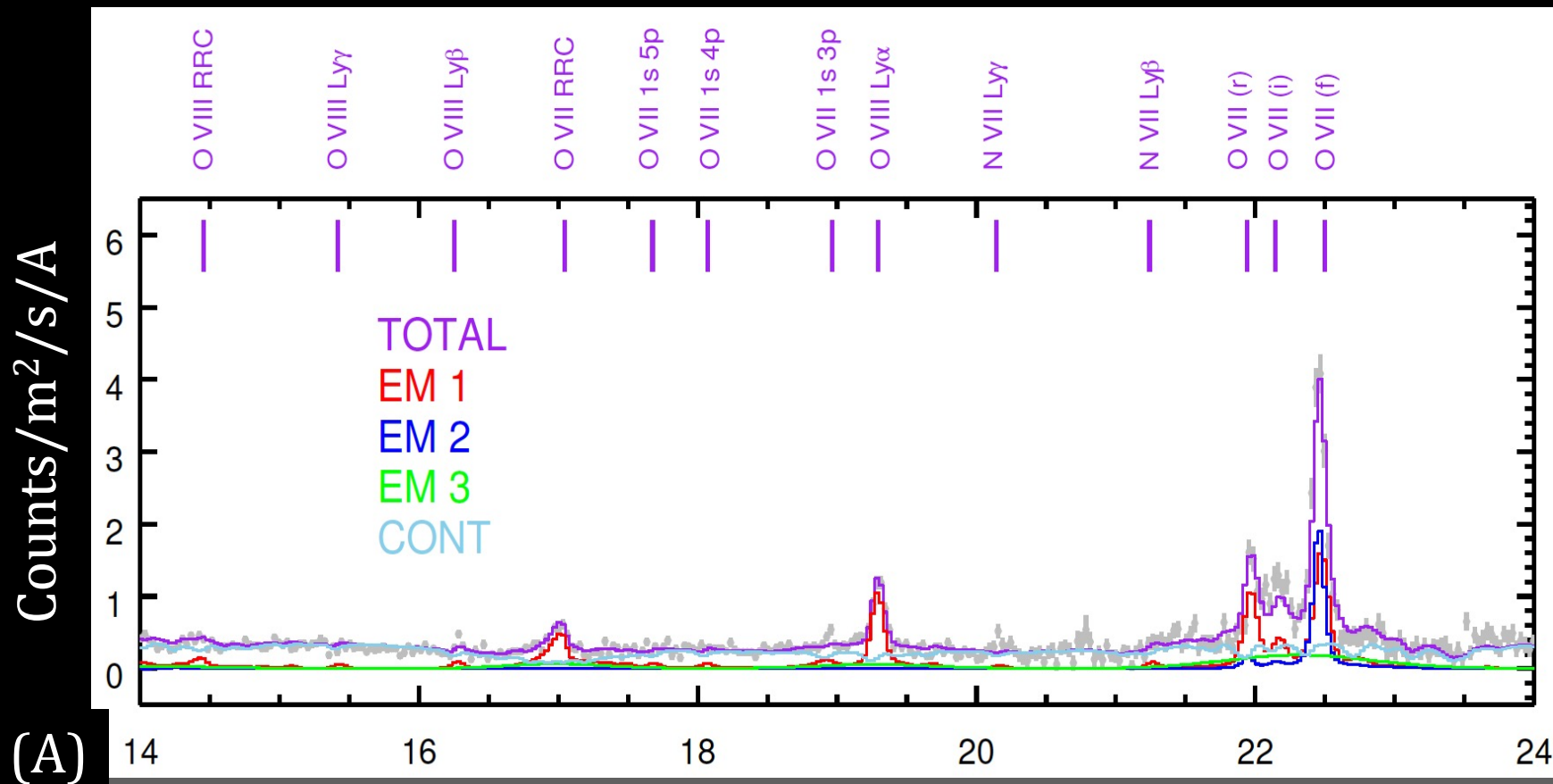
Whewell et al. 2015

- $r_{\text{ELR}} = 13.9 \text{ pc}$

Ebrero et al. 2016

- $r_{\text{WA}} = 5 - 10 \text{ pc}$

RGS Spectrum 2013;
J. Mao et al. 2017

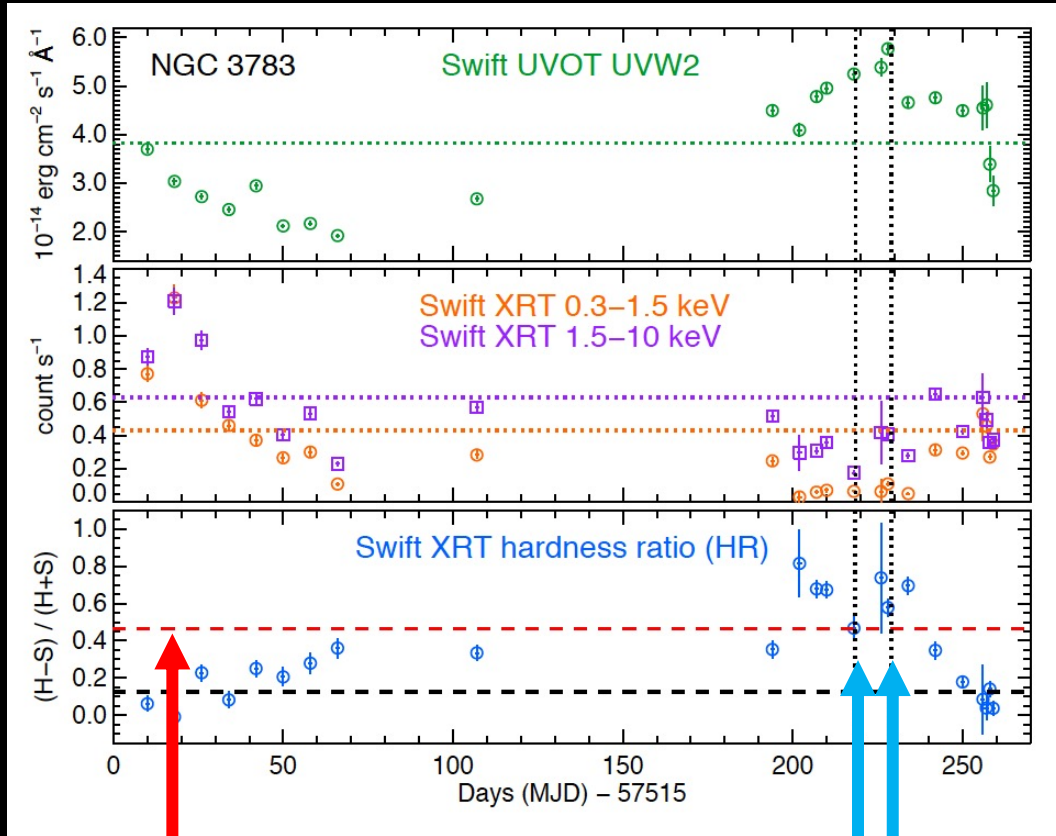


NGC 3783



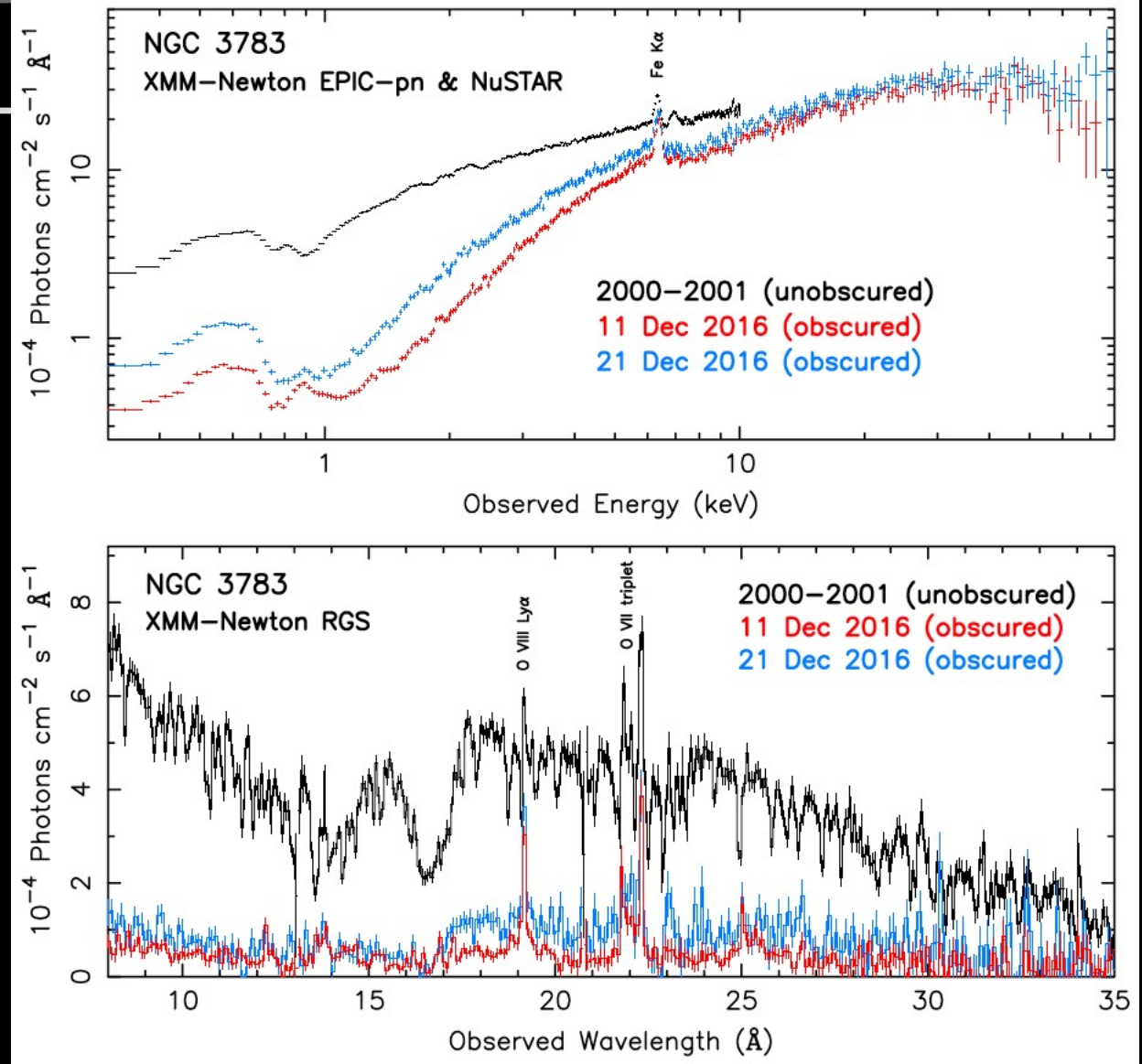
DSS; Simbad

Swift Triggering



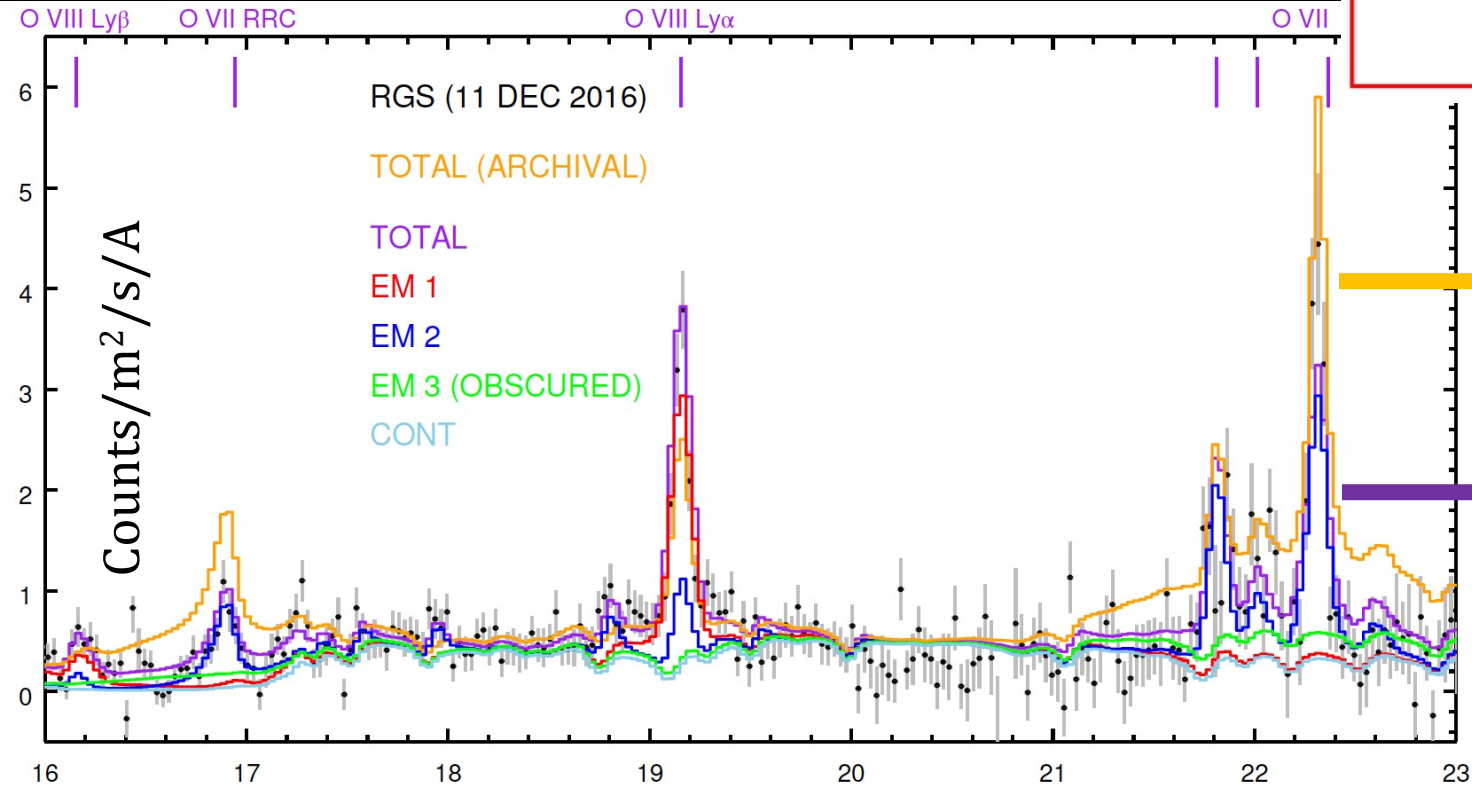
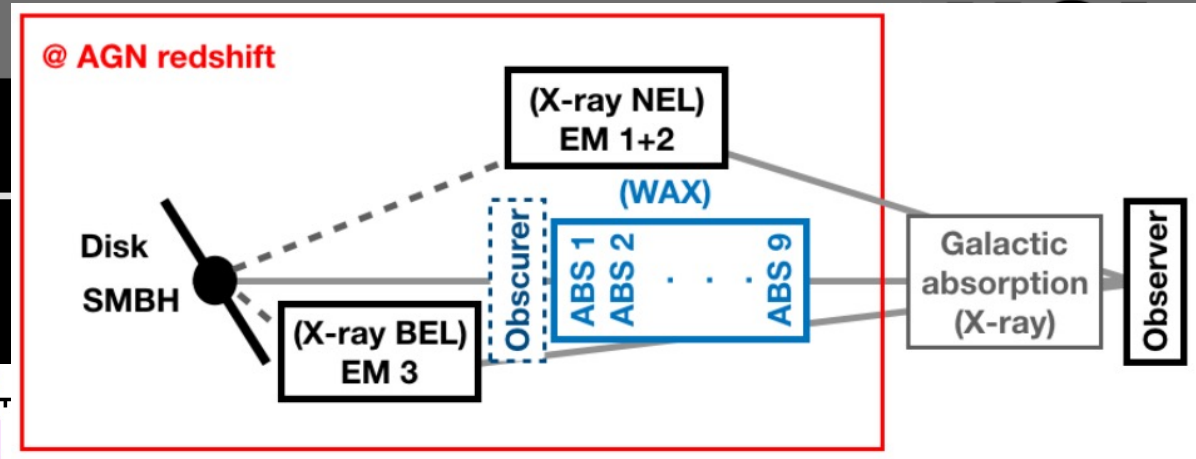
Hardness ratio triggering limit

Observations with XMM, NuSTAR and HST



M. Mehdipour et al. 2017

Multiple Emission Components



Comp.	N_H 10^{26} m^{-2}	$\log_{10}(\xi)$ 10^{-9} W m	v_{mic} km s^{-1}	C_{em} %	E.M. 10^{70} m^{-3}
2000–2001					
1	60 ± 37	2.60 ± 0.07	600 ± 100	0.29 ± 0.12	$0.5^{+0.8}_{-0.4}$
2	$5.2^{+5.4}_{-2.3}$	1.35 ± 0.05	140^{+50}_{-100}	$0.6^{+0.4}_{-0.2}$	$1.5^{+4.1}_{-1.0}$
3	28^{+72}_{-5}	0.82 ± 0.02	100 (f)	$0.3^{+0.1}_{-0.2}$	13^{+53}_{-10}
11 DEC 2016					
1	25 ± 6	2.58 ± 0.05	590 ± 90	0.98 ± 0.13	$1.0^{+0.6}_{-0.4}$
2	3.0 ± 0.7	1.03 ± 0.05	350 ± 70	7.0 ± 1.3	30^{+19}_{-13}
3	28 (f)	1.00 (f)	100 (f)	0.3 (f)	13 (f)

Wavelength (Å)

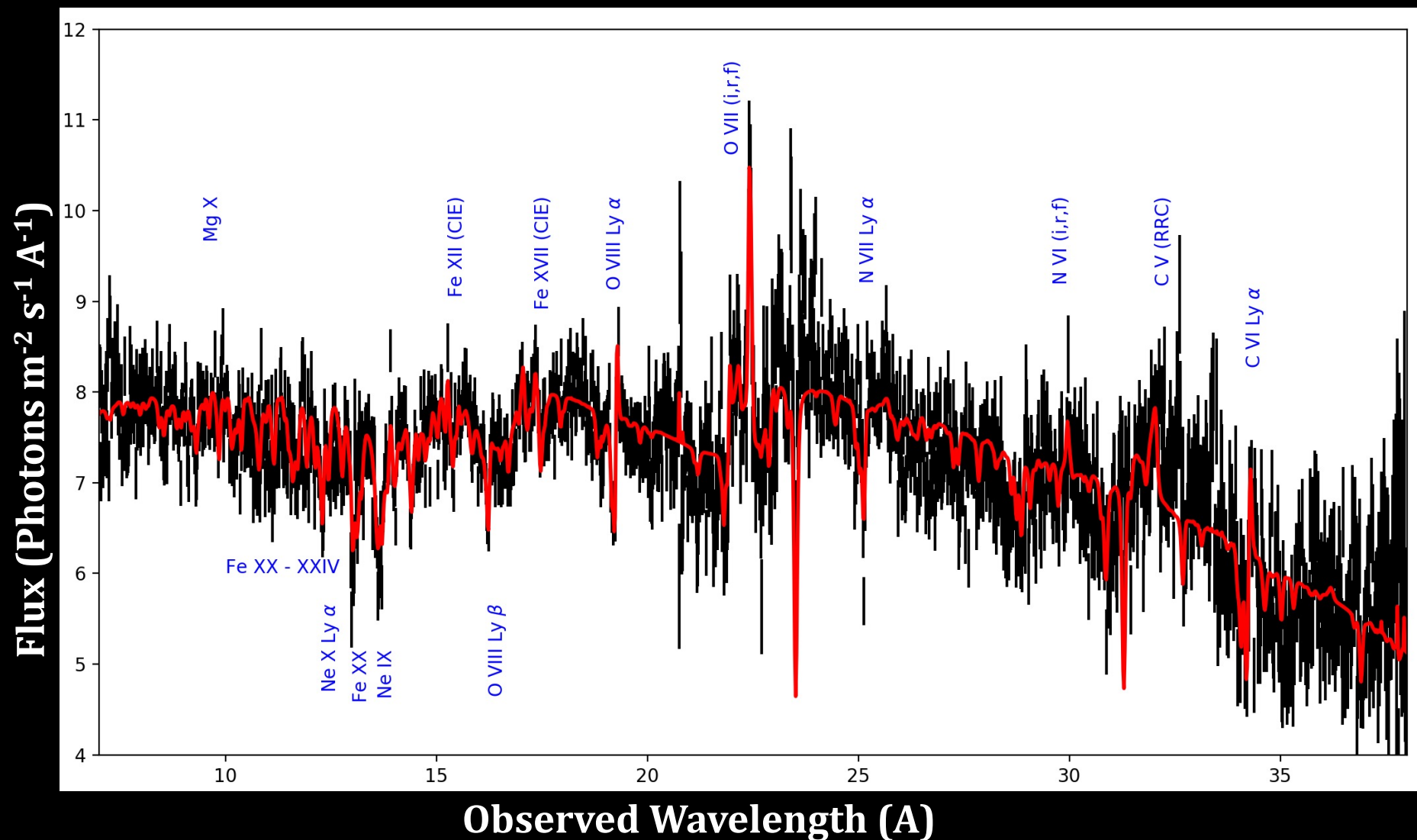
J. Mao et al. 2018

NGC 7469



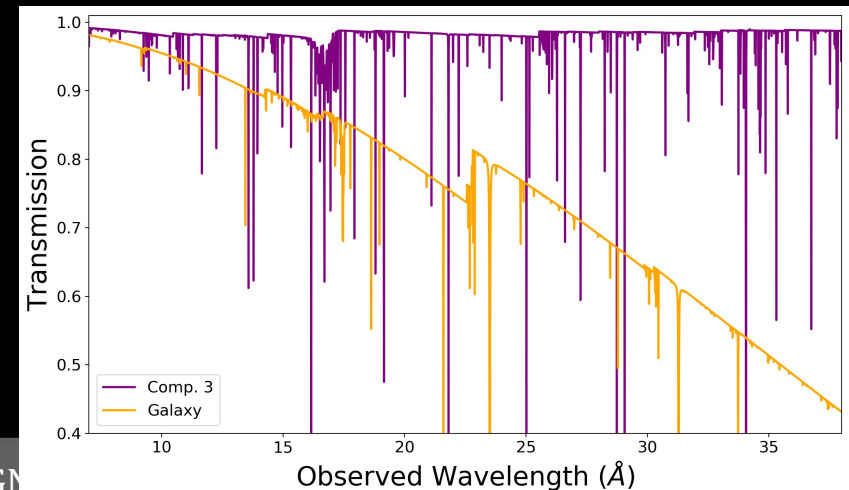
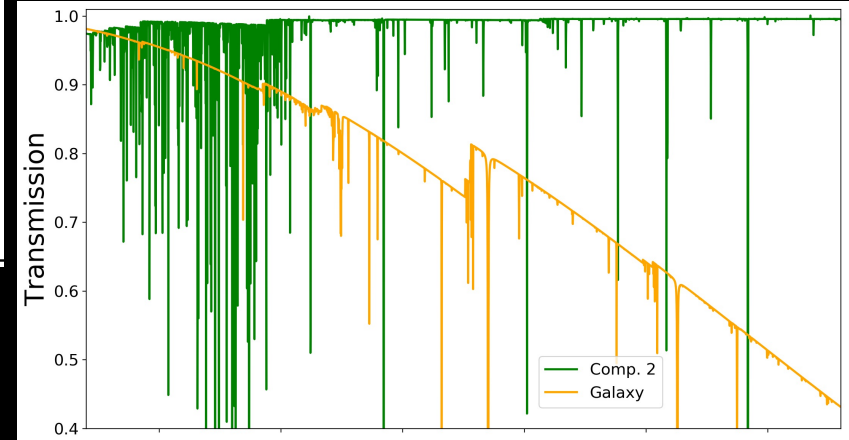
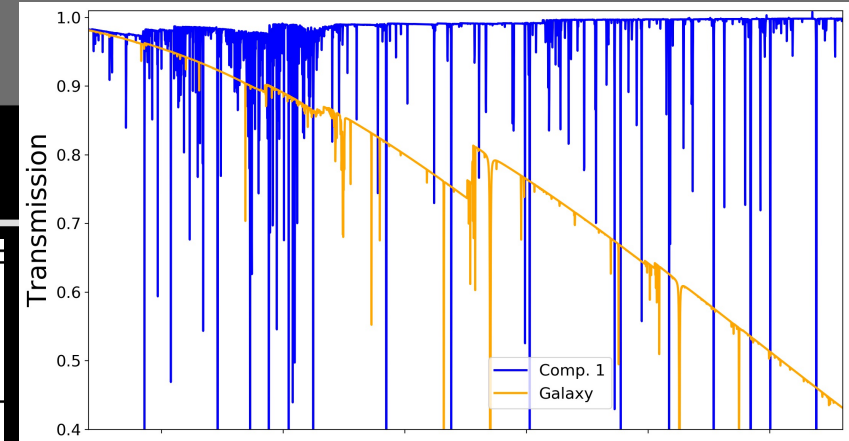
NASA/ESA/Hubble

RGS Analysis – Our Contribution



The Warm Absorber

Absorption Component	N_H (10^{24} m^{-2})	$\log \xi$ (10^{-9} Wm)	v_{turb} (km s^{-1})	v_{out} (km s^{-1})
\rightarrow 1	$10.0^{+0.5}_{-0.4}$	2.32 ± 0.01	35 ± 2	-630 ± 20
\rightarrow 2	52.0 ± 2.2	3.00 (f)	$a -$	-910^{+50}_{-30}
\rightarrow 3	2.3 ± 0.1	1.57 ± 0.04	11 ± 3	-1960 ± 20



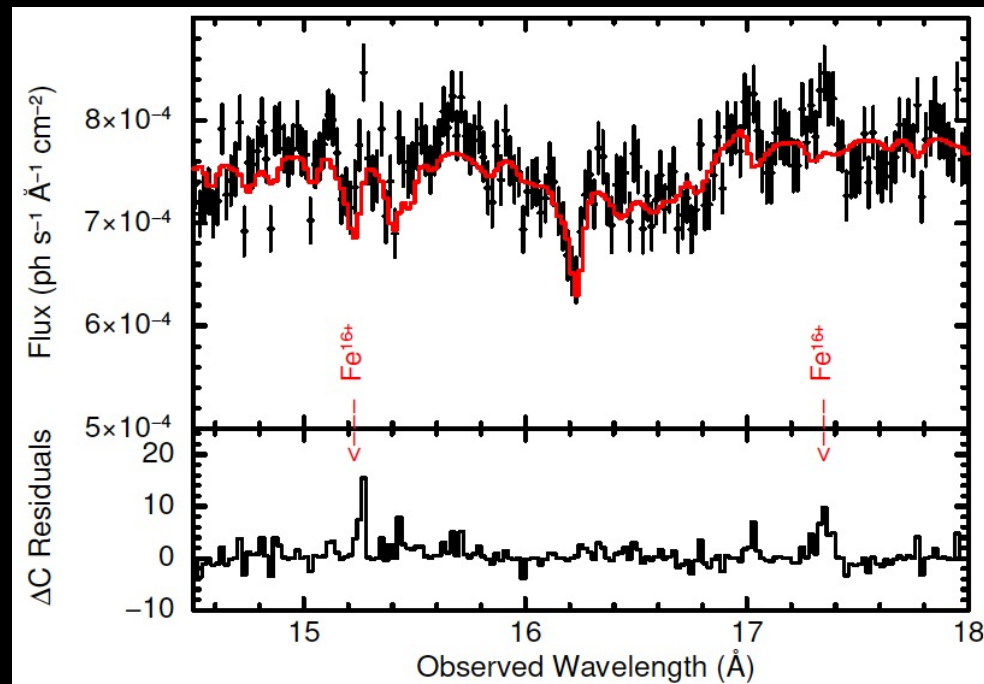
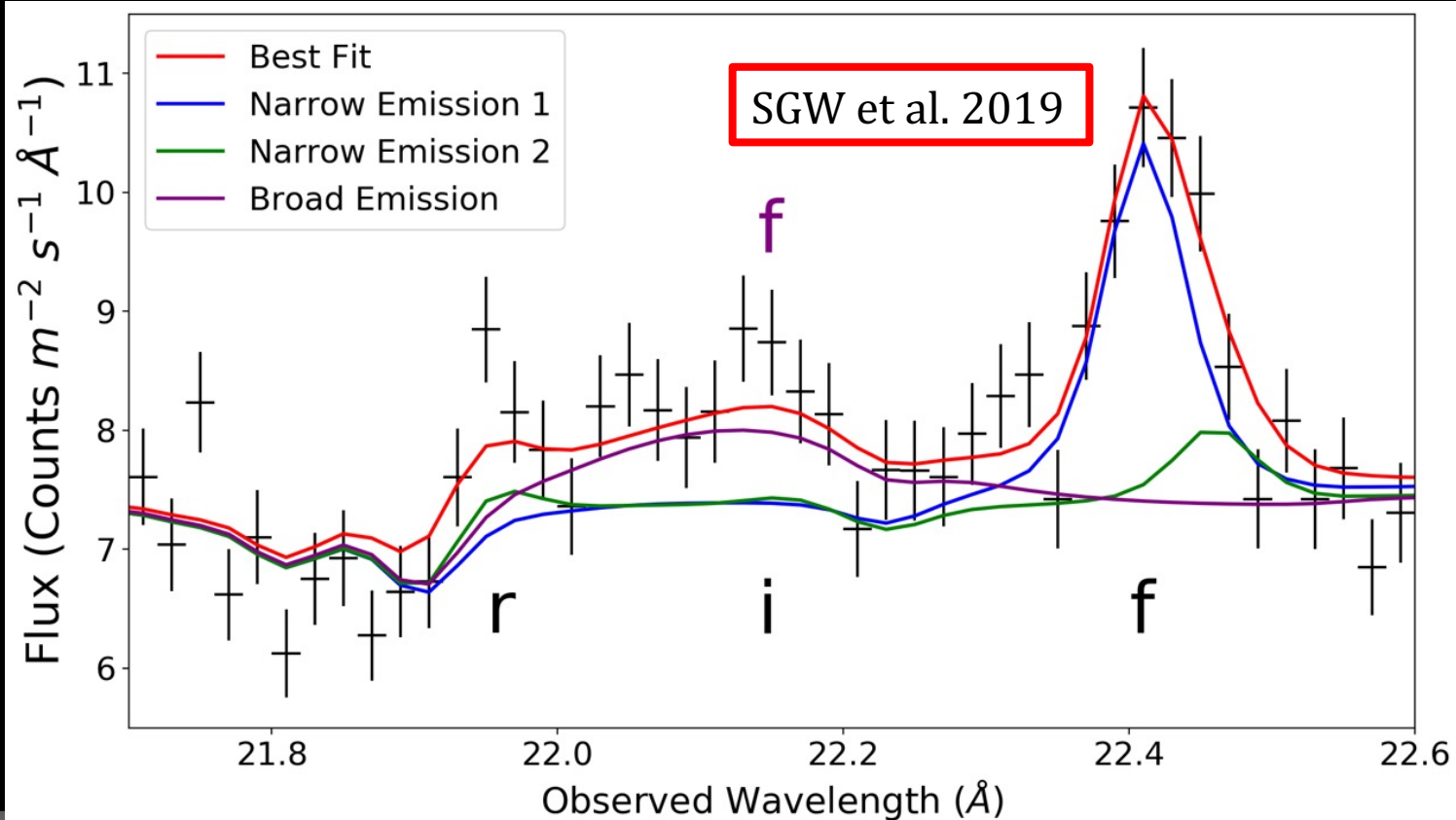
Comp. #	v_{out}^a (km s^{-1})	v_{turb} (km s^{-1})	$\log \xi$ ($\text{erg s}^{-1} \text{ cm}$)	N_H (10^{20} cm^{-2})	ΔC
1	-650 ± 50	70 ± 10	-0.6 ± 0.2	0.2 ± 0.1	33
2	...	70 ± 10	1.4 ± 0.1	1.0 ± 0.3	221
\rightarrow 3	...	70 ± 10	2.0 ± 0.1	5.5 ± 1.0	1027
\rightarrow 4	-950^{+50}_{-100}	35 ± 20	2.7 ± 0.2	22 ± 10	383
\rightarrow 5	-2050^{+50}_{-160}	60 ± 30	2.0 ± 0.3	1.1 ± 0.3	82
6	...	60 ± 30	0.3 ± 0.2	0.1 ± 0.1	48

SGW et al.
2019

E. Behar et
al. 2017

Emission Line Regions

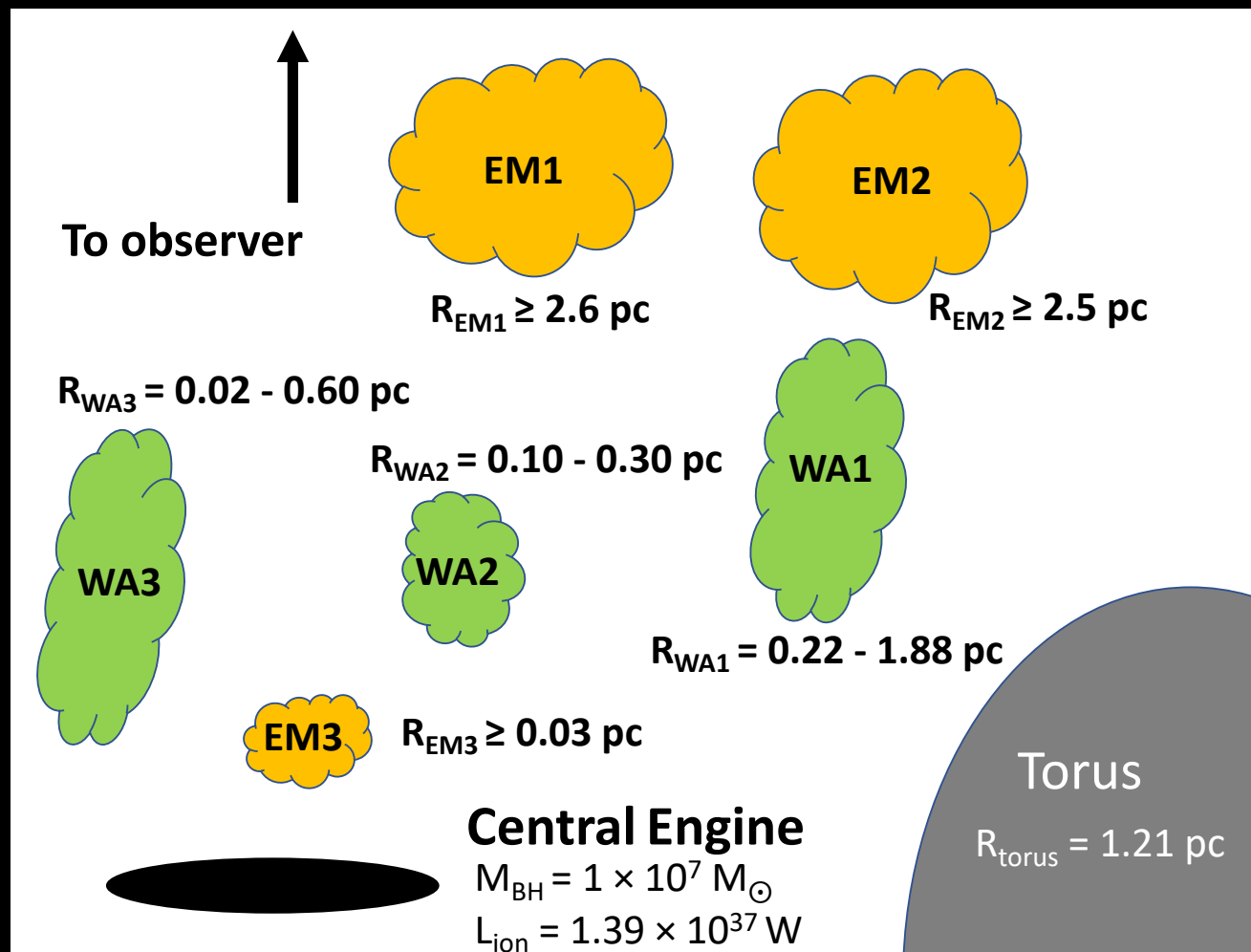
Emission Component	N_H (10^{25} m^{-2})	$\log \xi$ (10^{-9} Wm)	v_{turb} (km s^{-1})	v_{out} (km s^{-1})	$C_{cov} = \Omega/4\pi$
→ EM1	641 ± 50	$0.35^{+0.09}_{-0.01}$	50^{+140}_{-50}	-660^{+110}_{-20}	$2.1 \pm 0.2 \times 10^{-4}$
→ EM2	42^{+7}_{-6}	1.55 ± 0.08	50^{+180}_{-30}	0 (f)	$2.1 \pm 0.3 \times 10^{-3}$
→ EM3	787^{+130}_{-110}	$0.18^{+0.01}_{-0.07}$	$^a 1360^{+340}_{-270}$	-4460^{+200}_{-110}	$1.4 \pm 0.2 \times 10^{-4}$



E. Behar et al. 2017

Location of ELR

f = volume filling factor



$$r_{\min} = \frac{L_{\text{ion}} f}{N_H \xi}$$

$$N_H = \int_{r_{\min}}^{r_{\max}} n f dr$$

$$\xi \equiv \frac{L_{\text{ion}}}{n r^2}$$

Assume:

- Extended regions
- No further absorption by WA

Values for f

- Require f value < 1
 - $f \sim 0.01$ for most nebulae (e.g. Osterbrock 1991).
 - $f \sim 0.001$ for BLR (e.g. Sneddon & Gaskell 1999).
- For EM1 and EM2 we assume $f = 0.1$
- For EM3 $f = 0.001$

Emission Comp.	R (pc)
EM1	$2.62^{+0.31}_{-0.73}$
EM2	$2.52^{+1.05}_{-0.81}$
EM3	0.03 ± 0.01

However ...

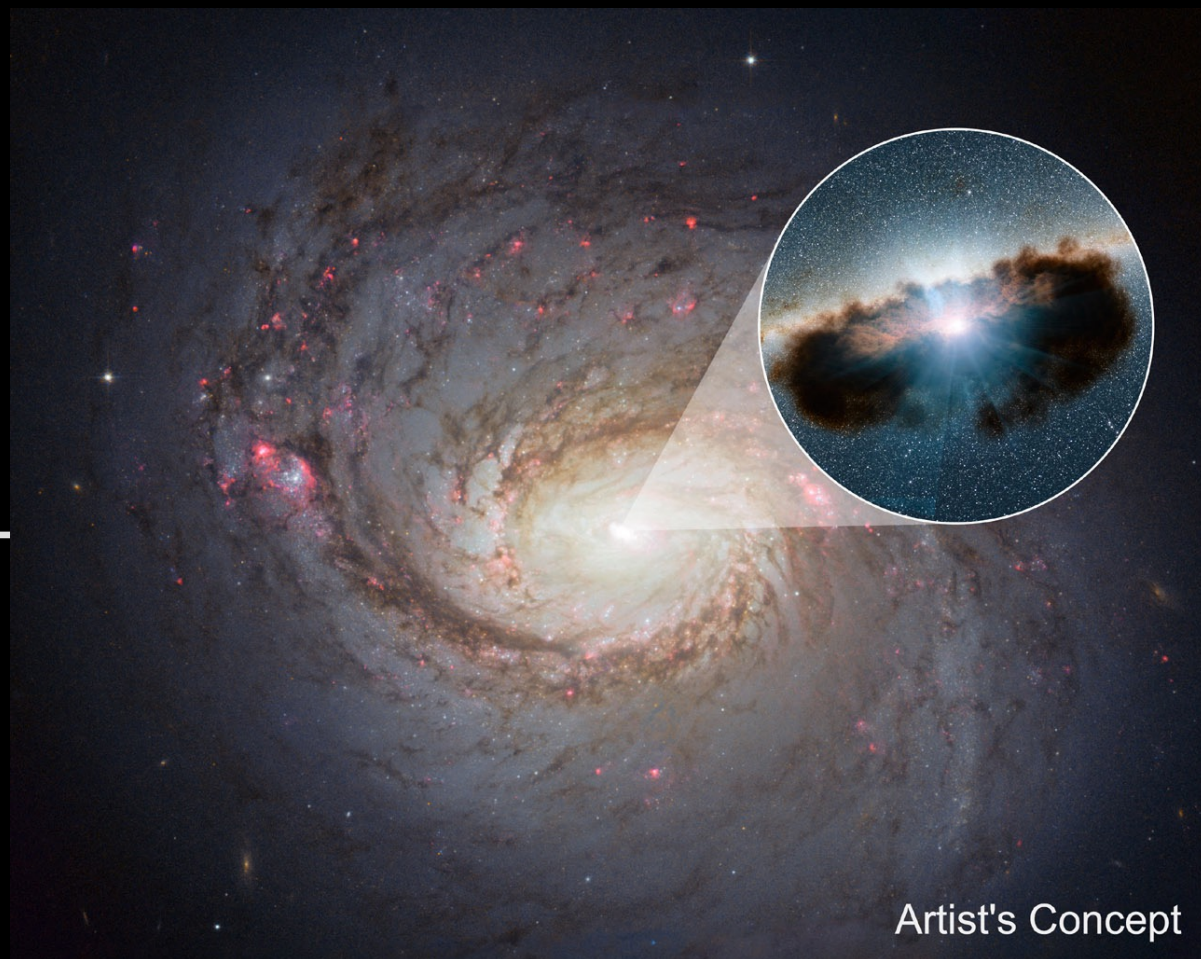
- Optical BLR $r_{\text{BLR}} = 0.004 \text{ pc}$ (Kollatschny & Zetzl 2013).
- Kinematics: $v_{\text{esc}} = v_{\text{out}} \sim -4500 \text{ kms}^{-1}$ $\left(R = \frac{2GM_{\text{BH}}}{v_{\text{out}}^2} \right)$
 - $r_{\text{EM3}} \simeq 0.004 \text{ pc}$.
- Possible solution: $f_{\text{EM3}} < 0.001$
- But most likely due to ξ of EM3

$$r_{\text{min}} = \frac{L_{\text{ion}} f}{N_{\text{H}} \xi}$$

Conclusions for NGC 7469

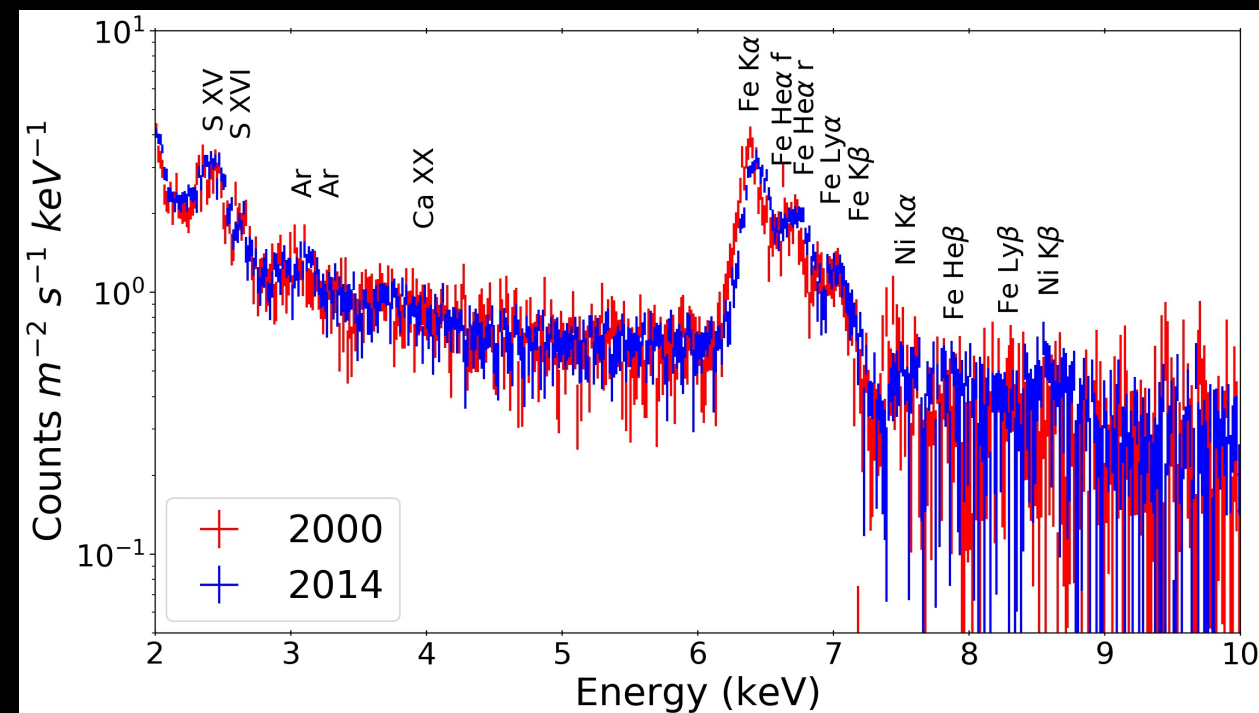
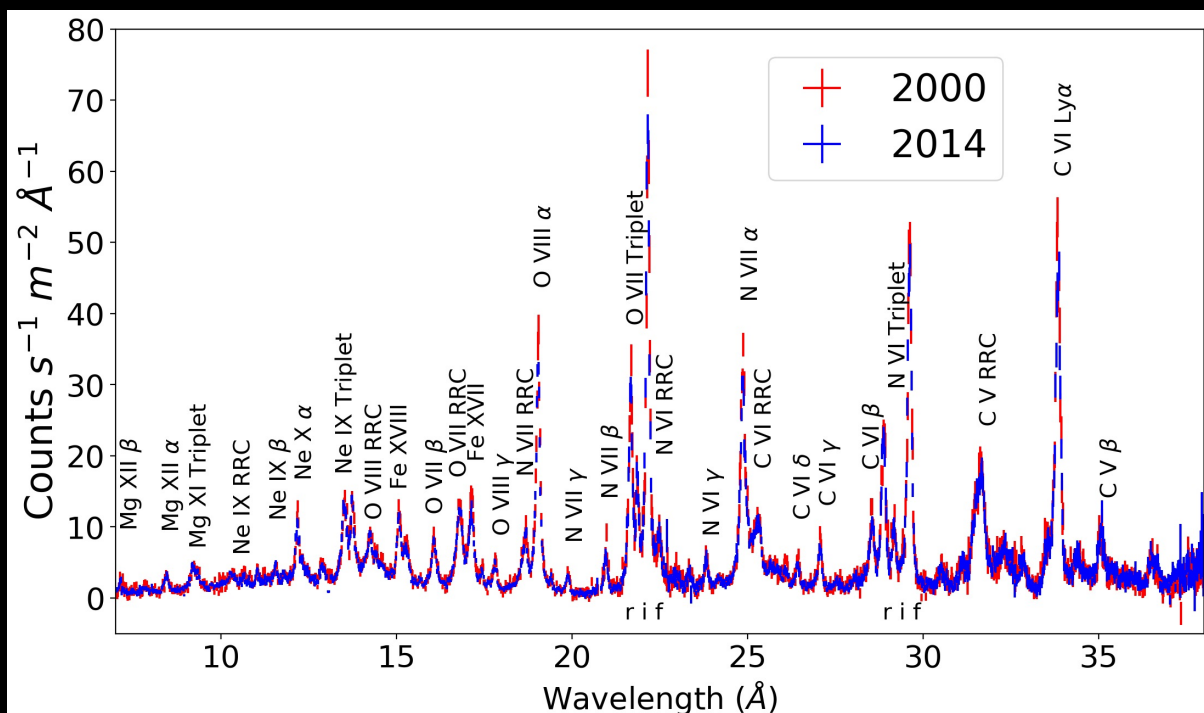
- WA can be explained by 3 components – different N_{H} , v_{out} , ξ
- Most emission lines are fitted with 2 narrow emission components
- Able to measure the distances of the Narrow Line Region
 - Assuming no further absorption by the WA
- Some lines require a broad component
 - Uncertain if it is a physical component

NGC 1068



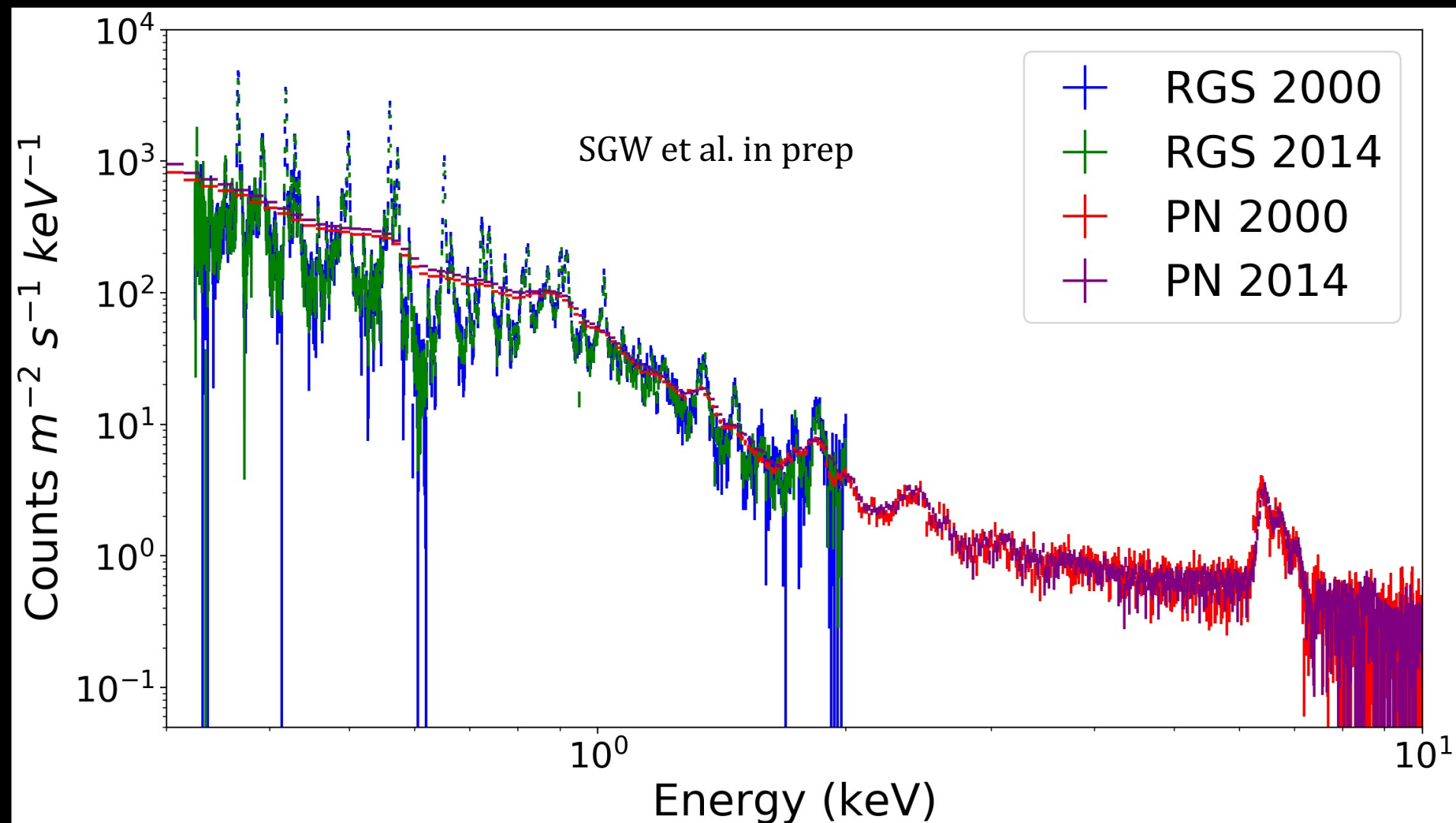
NASA/JPL-Caltech

XMM-Newton Spectra of NGC 1068



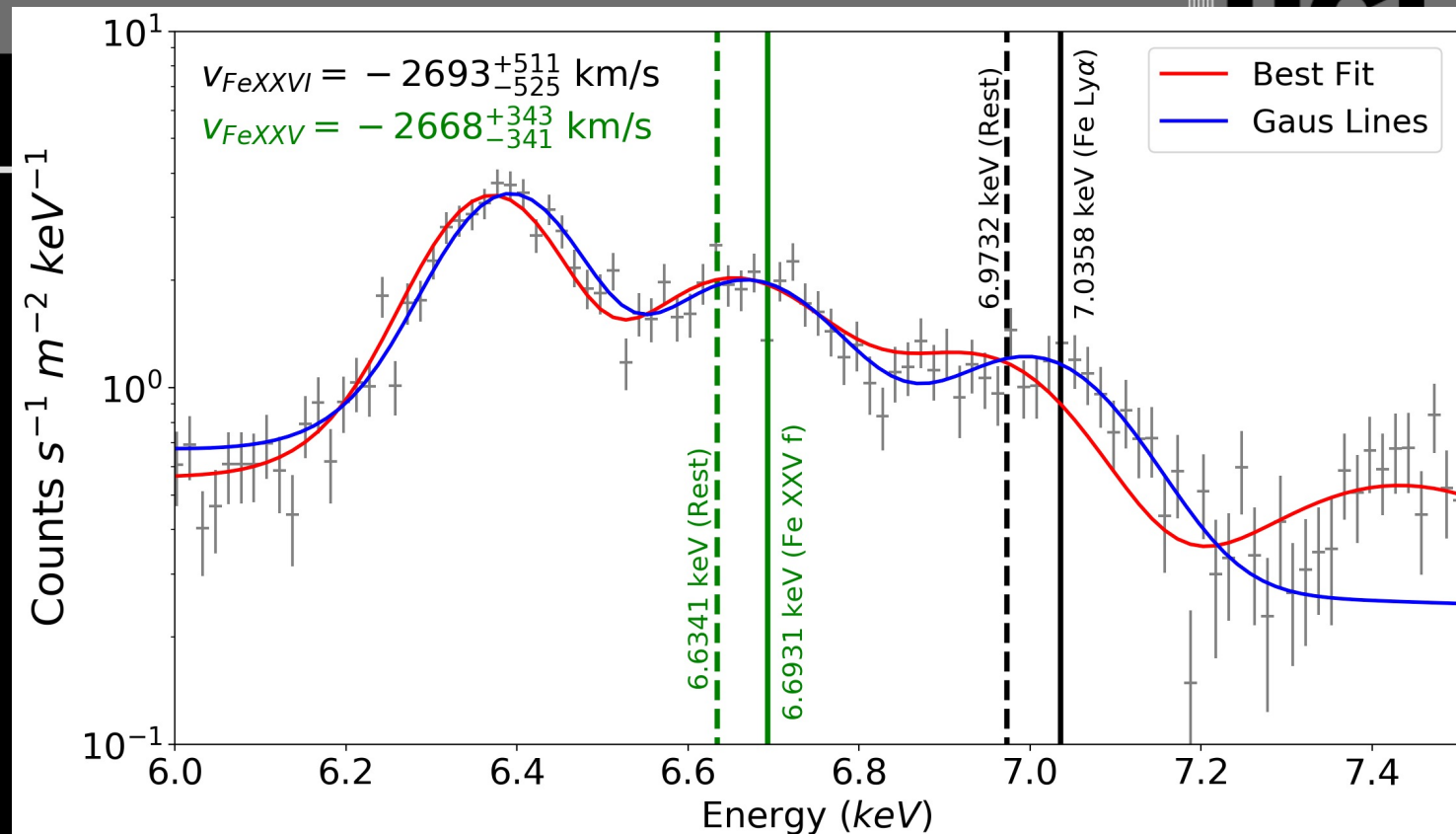
SGW et al. in prep

Simultaneous Fitting



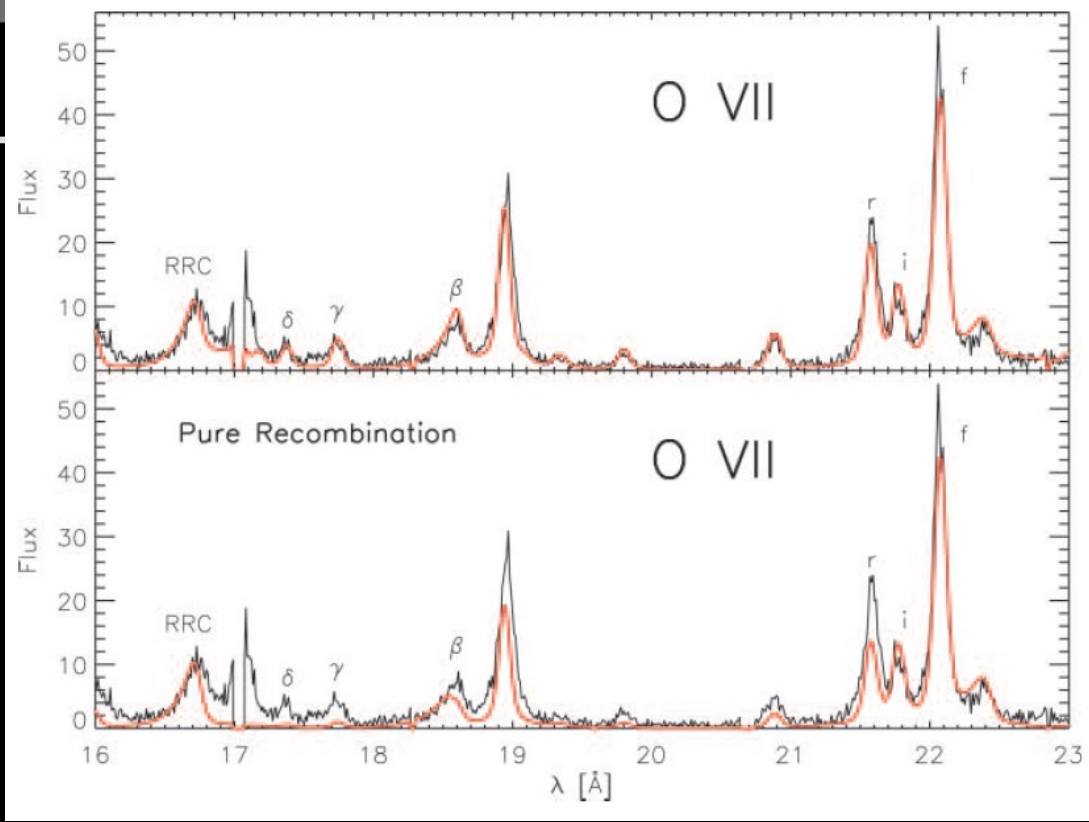
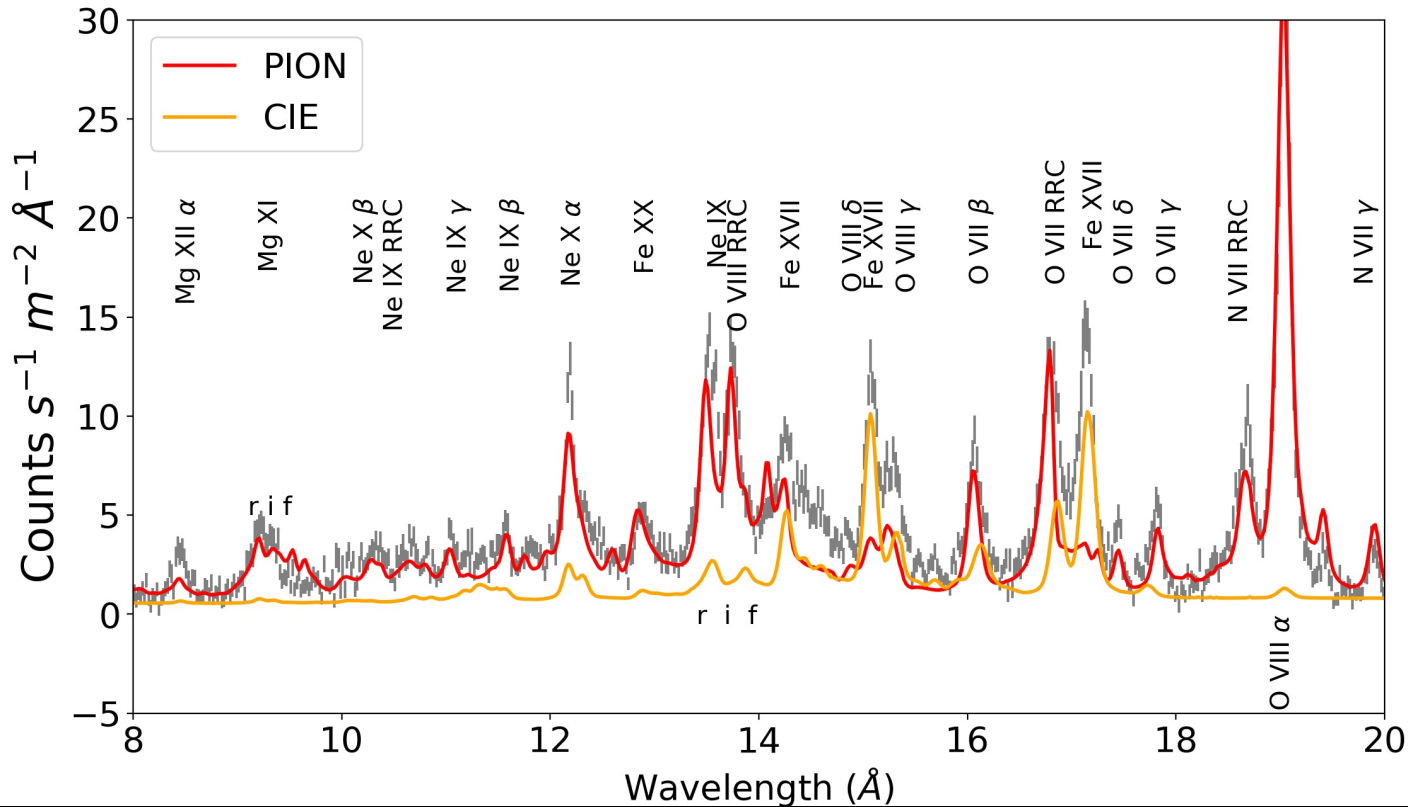
High Energy Lines

- Expect high energy component to be moving faster than lower two
- Find (with Gaussian components) that lines are blueshifted ~ 2680 km/s
- Therefore fix PION at this velocity
- Find a fourth component is required to solve this problem



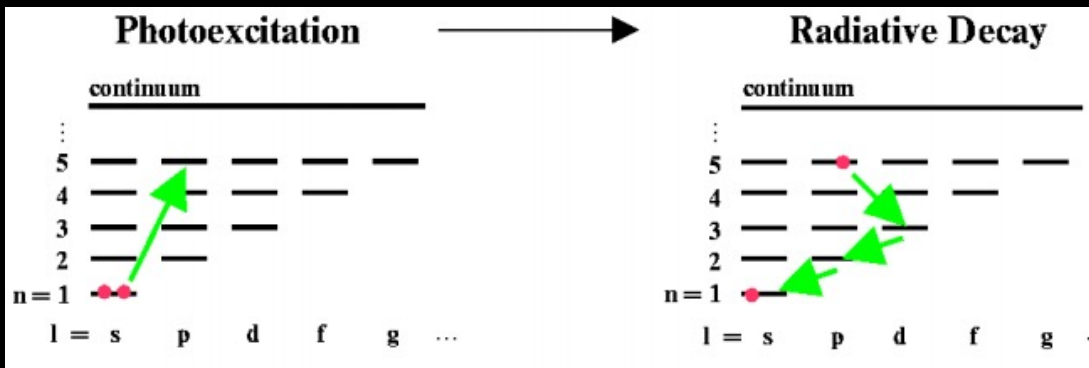
Obs.	PION Component	N_H (10^{25} m^{-2})	$\log \xi$ (10^{-9} W m)	v (km s^{-1})	v_{out} (km s^{-1})	$C_{cov} = \Omega/4\pi$
2000	EM1	130 ± 30	$3.82^{+0.01}_{-0.02}$	$3600^{+330}_{-240} \text{ }^a$	-75^{+86}_{-216}	$0.13^{+0.07}_{-0.06}$
	EM2	37^{+1}_{-4}	0.69 ± 0.01	$400 \pm 10 \text{ }^b$	-260 ± 10	$3.77 \pm 0.10 \times 10^{-2}$
	EM3	21 ± 2	$1.97^{+0.03}_{-0.01}$	$888 \pm 20 \text{ }^b$	-150^{+50}_{-5}	$5.64^{+0.92}_{-0.31} \times 10^{-2}$

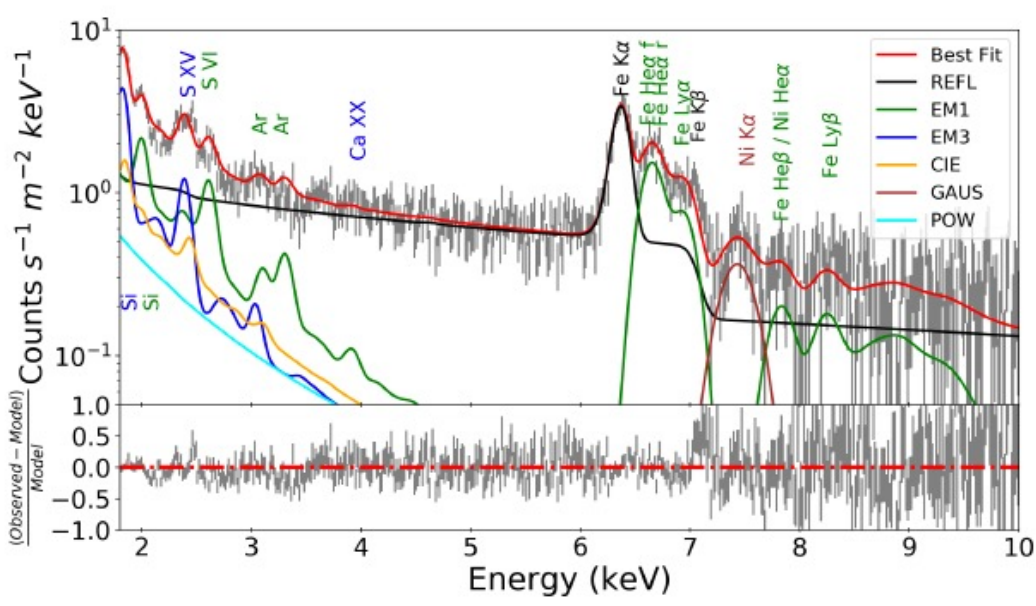
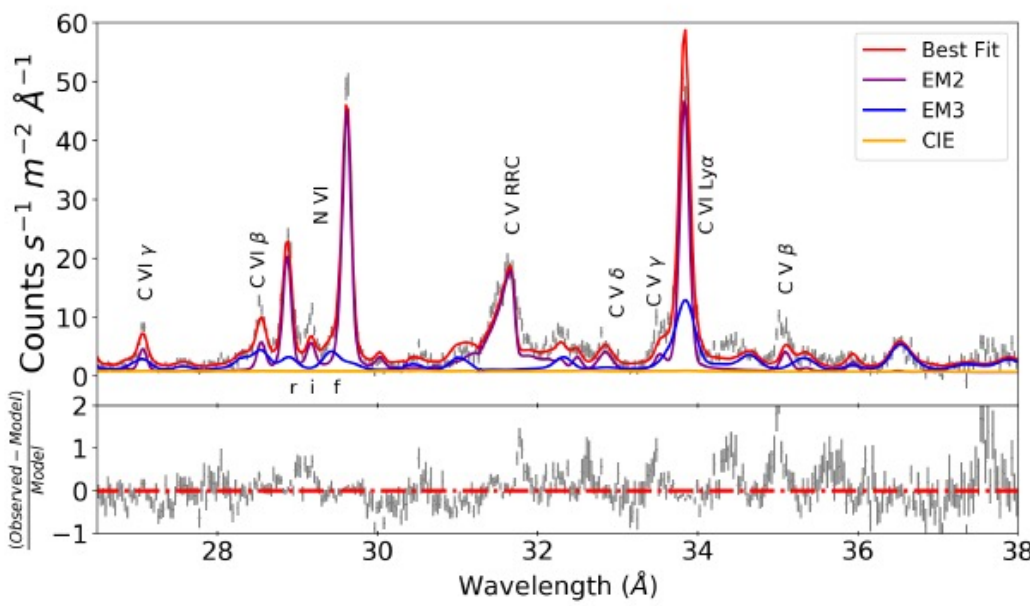
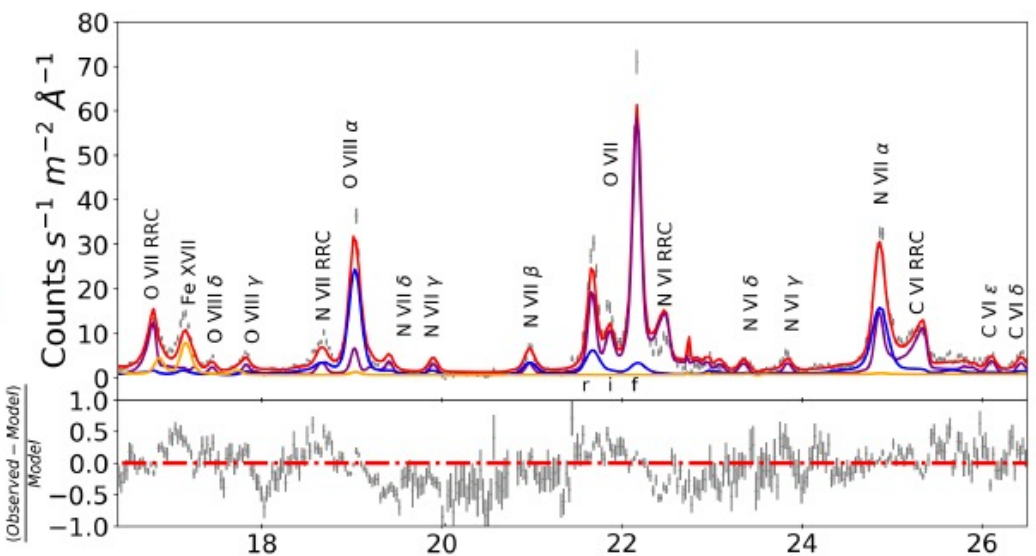
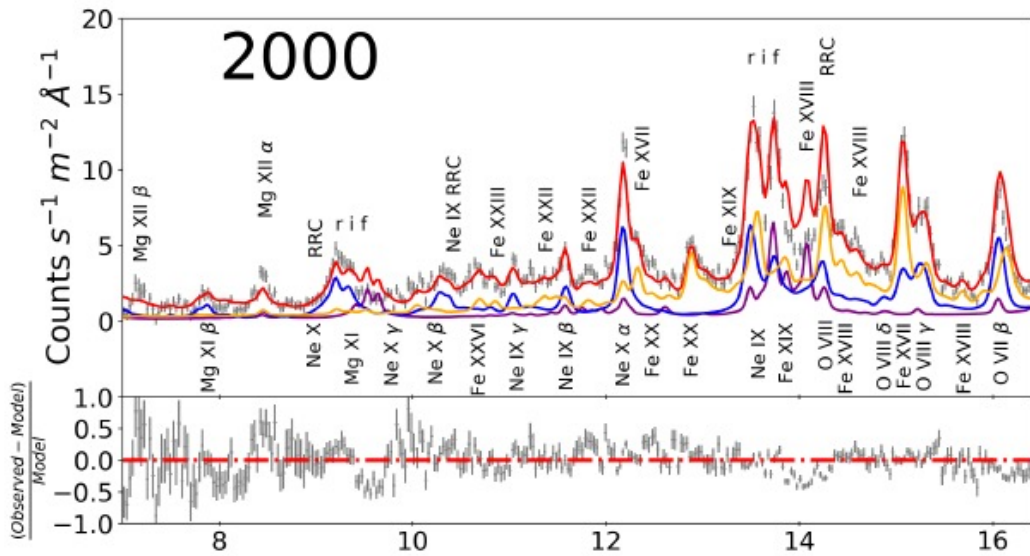
Collisionally Ionised Plasma



A. Kinkhabwala et al. 2002

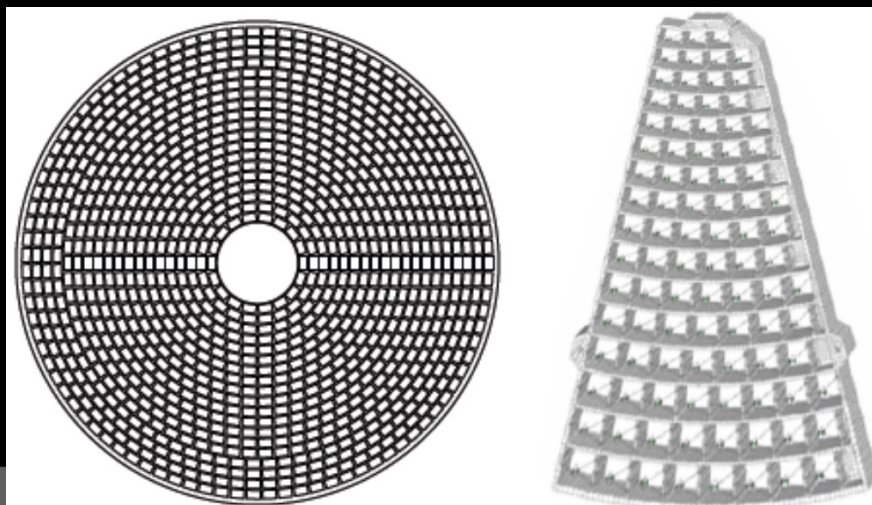
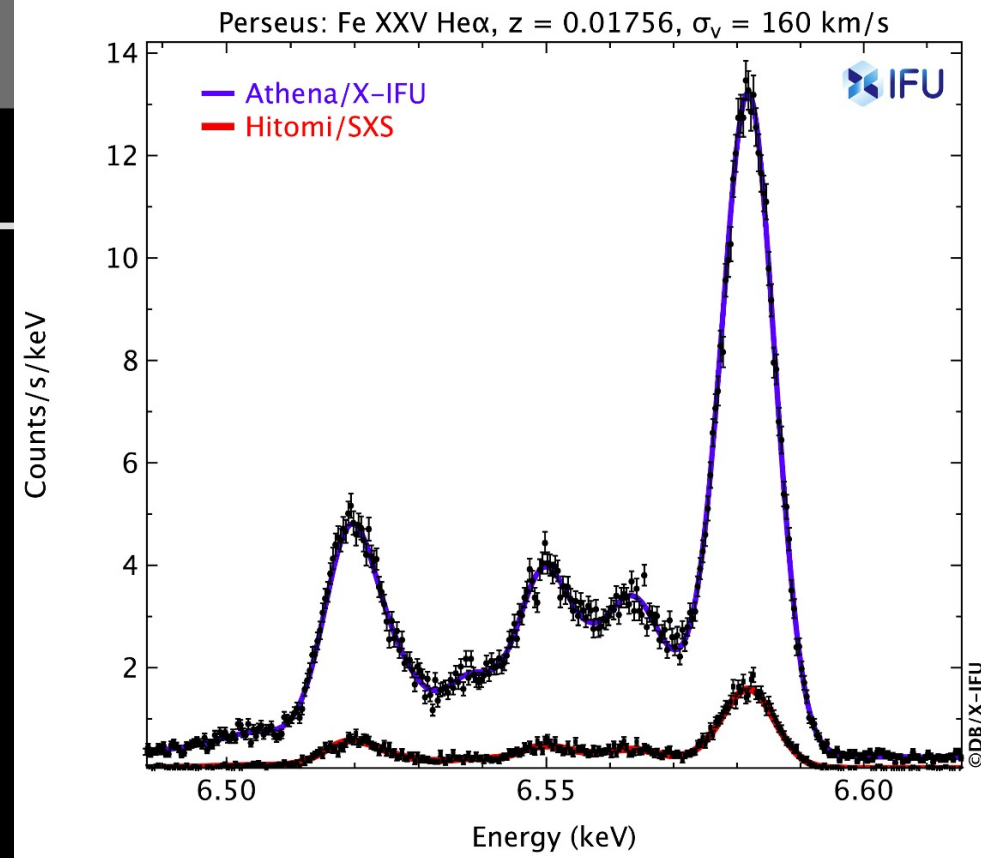
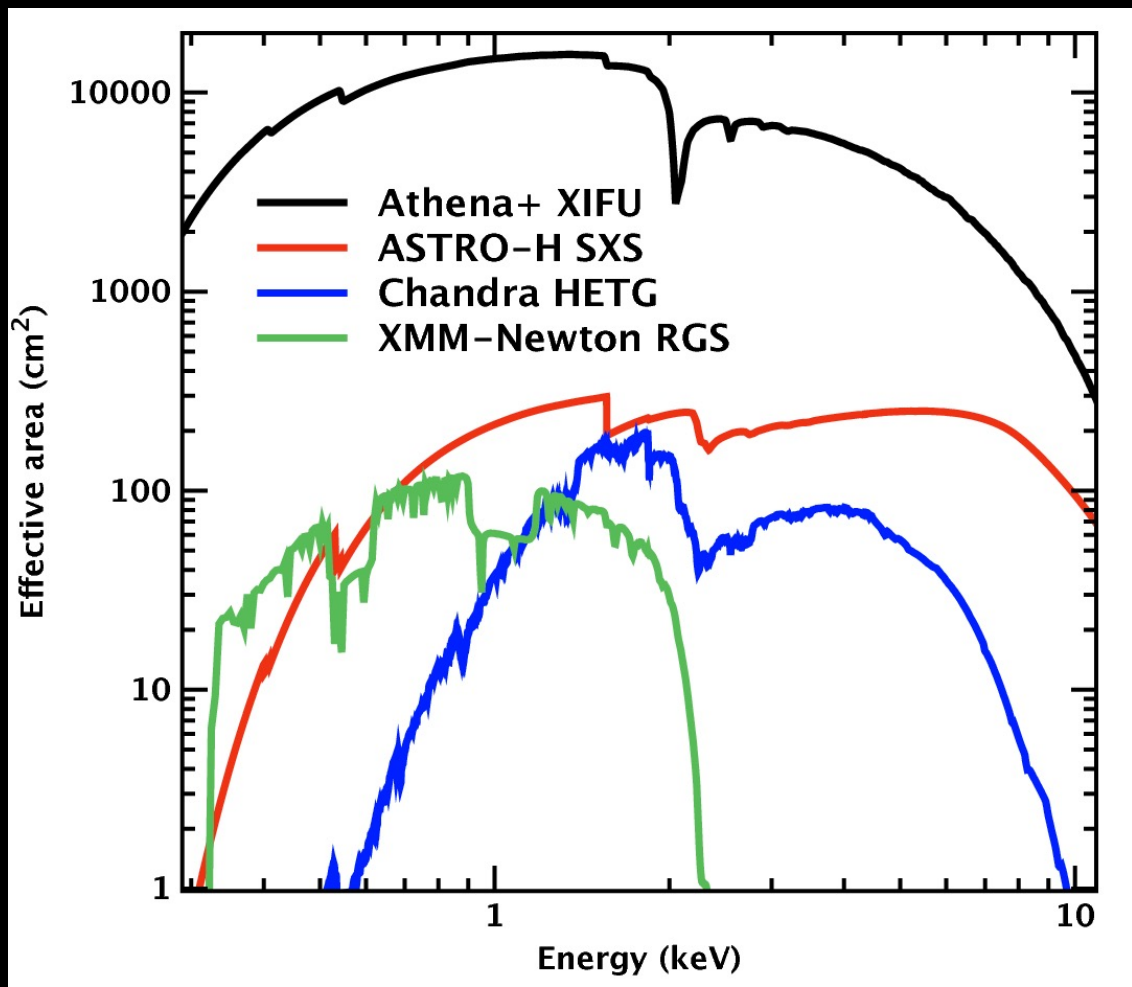
SGW et al. in prep





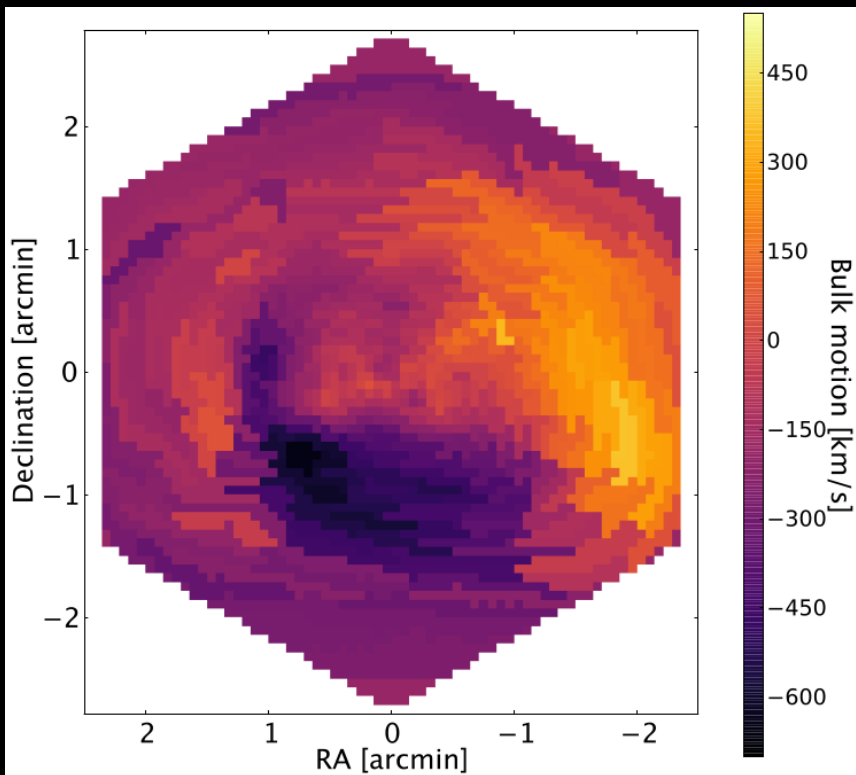
Looking into the Future

ATHENA



X-IFU consortium: Barrett et al. 2013; Nandra et al. 2013; Willingale et al. 2013

X-IFU (X-ray integral field unit)



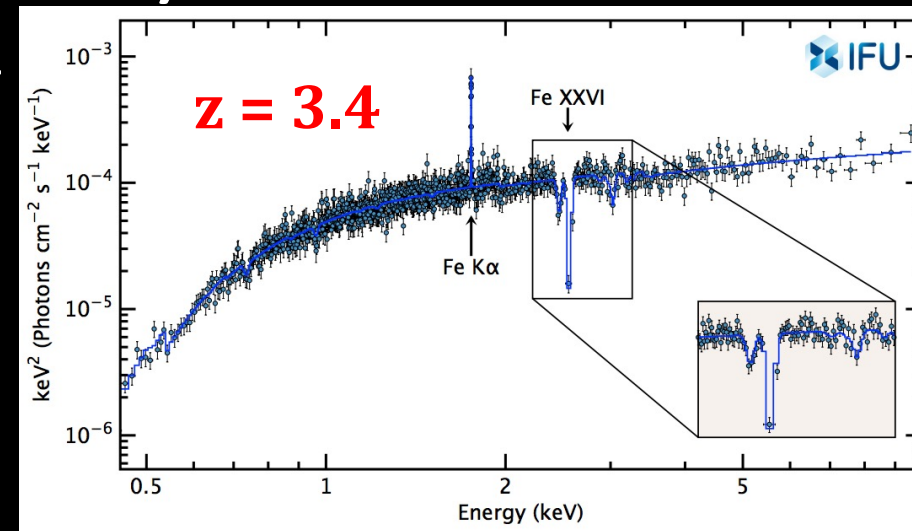
Hyper-luminous quasar
50 ks spectrum

UFO:

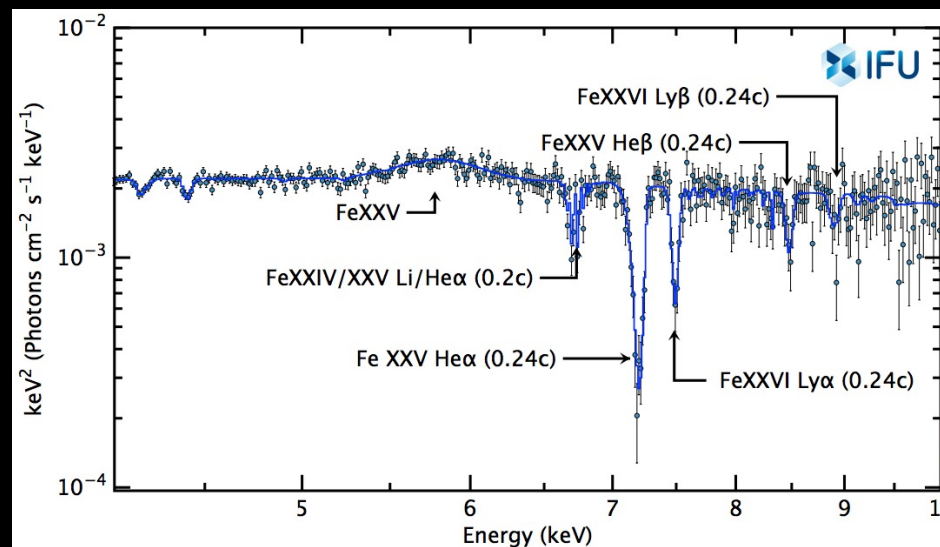
- $v_{\text{out}} = 0.15 c$

$$\Delta T \propto E_{Xray}$$

X-IFU team
(E. Cucchetti,
IRAP)



	RGS	X-IFU
Energy Range (keV)	0.3 - 2.5	0.2 - 12
Resolution (eV)	2 - 6	2.5 (@ 7 keV)



X-IFU team (Barrett 2019)

PDS456 ($z = 0.184$)
Simulated 100 ks

UFO:

- $\log \xi = 3.1, 3.6$

Summary

- High resolution X-ray spectroscopy and photoionisation modelling are tools to study highly ionised plasma regions within AGN
- Obtaining distances and parameter measurements of the ELR help to relate it to the WA and outflowing winds
- Recent obscuring events in Seyfert 1 AGN require further investigation
- Outflowing plasma regions will aid us in understanding how AGN and the host galaxy co-evolve through feedback
- Athena will allow for more accurate high resolution X-ray spectra across the full energy band